Genetic interactions of hypomorphic mutations in the m^{7}G cap-binding pocket of yeast nuclear cap binding complex: An essential role for Cbc2 in meiosis via splicing of *MER3* pre-mRNA

ZHICHENG R. QIU,[1] LIDIA CHICO,[2] JONATHAN CHANG,[1] STEWART SHUMAN,[1,3] and BEATE SCHWER[2,3]

[1]Molecular Biology Program, Sloan-Kettering Institute, New York, New York 10065, USA
[2]Department of Microbiology and Immunology, Weill Cornell Medical College, New York, New York 10065, USA

ABSTRACT

Nuclear cap binding protein complex (CBC) is a heterodimer of a small subunit (Cbc2 in yeast) that binds the m^{7}G cap and a large subunit (Sto1 in yeast) that interacts with karyopherins. In order to probe the role of cap recognition in yeast CBC function, we introduced alanine mutations (Y24A, F91A, D120A, D122A, R129A, and R133A) and N-terminal deletions (NΔ21 and NΔ42) in the cap-binding pocket of Cbc2. These lesions had no effect on vegetative growth, but they ameliorated the cold-sensitivity of *tgs1*Δ cells that lack trimethylguanosine caps (a phenotype attributed to ectopic association of CBC with the m^{7}G cap of the normally TMG-capped U1 snRNA), thereby attesting to their impact on cap binding in vivo. Further studies of the Cbc2-Y24A variant revealed synthetic lethality or sickness with null mutations of proteins involved in early steps of spliceosome assembly (Nam8, Mud1, Swt21, Mud2, Ist3, and Brr1) and with otherwise benign mutations of Msl5, the essential branchpoint binding protein. Whereas the effects of weakening CBC–cap interactions are buffered by other actors in the splicing pathway during mitotic growth, the *NΔ42* allele causes a severe impediment to yeast sporulation and meiosis. RNA analysis revealed a selective defect in the splicing of *MER3* and *SAE3* transcripts in *cbc2-NΔ42* diploids during attempted sporulation. An intronless *MER3* cDNA fully restored sporulation and spore viability in the *cbc2-NΔ42* strain, signifying that *MER3* splicing is a limiting transaction. These studies reveal a new level of splicing control during meiosis that is governed by nuclear CBC.

Keywords: cap recognition; U1 snRNP; branchpoint binding protein; meiosis; pre-mRNA splicing

INTRODUCTION

The m^{7}G cap structure is a signature feature of RNA polymerase II transcripts. The cap is formed by three enzymatic reactions that occur shortly after the 5′-triphosphate end of the nascent RNA is extruded from the polymerase elongation complex. The m^{7}G cap can exert a positive influence on downstream mRNA transactions such as splicing, polyadenylation, and nuclear export, and it is a decisive factor in translation initiation and mRNA stability (Topisirovic et al. 2011). Trimethylguanosine (TMG) cap structures are characteristic of the small nuclear (sn) RNAs that program mRNA splicing (U1, U2, U4, U5). TMG is formed post-transcriptionally by the enzyme Tgs1, which catalyzes two successive methyl additions to the N2 atom of the m^{7}G cap (Mouaikel et al. 2002; Hausmann and Shuman 2005). Whereas m^{7}G caps are essential for the viability of eukaryal cells, TMG caps are not (Mouaikel et al. 2002; Hausmann et al. 2007).

The effector functions of the m^{7}G cap are mediated by two dedicated cap binding proteins (Topisirovic et al. 2011). eIF4E is a predominantly cytoplasmic translation initiation factor that targets the 40S ribosomal subunit to the 5′ mRNA end. Most eukaryal translation is eIF4E-dependent, and the *CDC33* gene encoding *Saccharomyces cerevisiae* eIF4E is essential for viability. A nuclear cap binding protein complex (CBC) was identified initially in human cells and shown to play a role in pre-mRNA splicing

[3]**Corresponding authors**
E-mail bschwer@med.cornell.edu
E-mail s-shuman@ski.mskcc.org
Article published online ahead of print. Article and publication date are at http://www.rnajournal.org/cgi/doi/10.1261/rna.033746.112.

and U snRNA export (Izaurralde et al. 1994, 1995; Lewis et al. 1996). Metazoan CBC is a heterodimer of CBP80 and CBP20 subunits. The homologous yeast CBC subunits are Sto1 (861 aa) and Cbc2 (208 aa). CBC engages the m^7G caps of nascent RNA polymerase II transcripts, remains bound to them during cotranscriptional and post-transcriptional nuclear RNA processing, and then facilitates mRNA and snRNA export to the cytoplasm (Visa et al. 1996; Görnemann et al. 2005). Mammalian CBC bound to freshly exported mRNA can drive a pioneer round of translation before exchanging with eIF4E (Maquat et al. 2010).

Crystal structures of the CBP80/CBP20 heterodimer bound to cap analogs provide key insights to CBC function (Calero et al. 2002; Mazza et al. 2002). The cap-binding pocket resides wholly within the CBP20 subunit, which adopts a classical mixed α/β RRM fold. CBP80 (which has an all-α-helical tertiary structure) makes no contact with the cap, yet is required for cap binding by CBP20 because it interacts with the N-terminal peptide segment of CBP20 and stabilizes an active conformation of the cap-binding pocket. There are multiple atomic contacts between CBP20 amino acid side chains and the m^7G nucleoside, the triphosphate bridge, and 5′-terminal nucleobase of the RNA (Fig. 1). A key determinant of cap binding is the π-cation stack in which the positively charged m^7G base is sandwiched between two tyrosines (Tyr20 and Ty43 in human CBP20, corresponding to Tyr24 and Tyr49 in yeast Cbc2). Alanine substitutions of the proximal and distal tyrosines of CBP20 elicited 30-fold and 100-fold decrements in the affinity of CBC for m^7G-capped RNA (Mazza et al. 2002). In contrast, alanine mutation of the CBP20 tyrosine that stacks under the 5′ RNA nucleobase (the equivalent residue being a leucine in yeast Cbc2) did not affect the affinity of CBC for m^7G-capped RNA (Mazza et al. 2002).

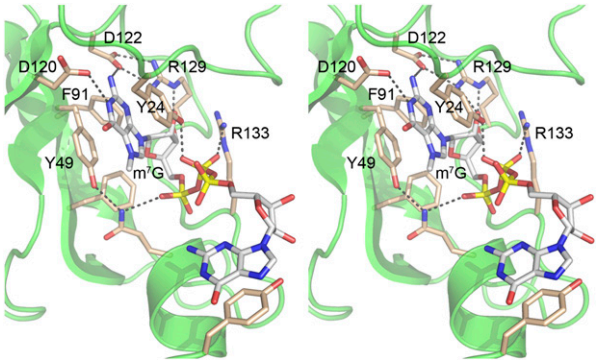

FIGURE 1. The cap-binding pocket of CBC. Stereo view of the CBP20 subunit of the human CBC (from pdb 1H2T) highlighting the π-cation stack of the m^7G cap nucleoside sandwiched between two conserved tyrosines and the hydrogen bonding contacts between conserved amino acid side chains and the m^7G base, the cap ribose, and the bridging phosphates of the cap dinucleotide. The amino acids are labeled in the figure according to their residue numbers in the homologous Cbc2 subunit of yeast CBC.

Despite the imputed centrality of CBC in mRNA and snRNA biogenesis, the genetics of CBC function are relatively uncharted. Yeast *sto1Δ* and *cbc2Δ* mutants are viable, but they grow slowly and display conditional phenotypes. *Arabidopsis* plants harboring T-DNA insertions that disrupt *CBP80* or *CBP20* are also viable, but they display reduced stature, serrated leaves, abscissic acid hypersensitivity, and enhanced drought tolerance (Hugouvieux et al. 2001; Papp et al. 2004). CBC functions in vivo have been inferred by characterizing RNA transactions in *sto1Δ* or *cbc2Δ* yeast strains (Colot et al. 1996; Fortes et al. 1999; Görnemann et al. 2005; Hossain et al. 2009) and in *cbp80* or *cbp20* mutant plants (Laubinger et al. 2008; Raczynska et al. 2010), but it is not clear whether the observed aberrations directly reflect the contributions of cap binding by CBC.

Here, we addressed this issue by surveying the effects of structure-guided mutations in the cap-binding pocket of yeast Cbc2. Subtracting many of the Cbc2 amino acids that contact the m^7G cap has no apparent impact per se on yeast growth, which suggests that (1) CBC's activities in vivo may not be limited to cap-dependent events, and/or (2) the contributions of high-affinity cap binding by CBC to RNA transactions may be buffered by other yeast proteins. We explored the latter scenario by gauging the genetic interactions of a hypomorphic *cbc2-Y24A* allele (that has no growth phenotype per se) with null alleles of otherwise inessential yeast proteins implicated in pre-mRNA splicing, and with otherwise benign mutations of the essential splicing factor Msl5. Our results highlight connections between yeast Cbc2, the U1 snRNP, and the branchpoint binding protein that fortify inferences about the role of CBC–cap interactions in spliceosome assembly.

We also report that a hypomorphic *cbc2-NΔ42* allele, which has no apparent effect on vegetative growth, impedes yeast sporulation and mimics the molecular lesion underlying the meiotically defective *sae1-1* mutant (McKee and Kleckner 1997). By surveying the splicing of meiotic pre-mRNAs in *cbc2-NΔ42* diploids undergoing attempted sporulation, we pinpointed the *MER3* and *SAE3* transcripts as being dependent on wild-type Cbc2 for efficient splicing. Genetic bypass of the *cbc2-NΔ42* sporulation defect by either *MER3* cDNA expression or the installation of a consensus 5′ splice site in the *MER3* intron illuminates a new role for nuclear CBC as a governor of gene-specific pre-mRNA splicing during meiotic development.

RESULTS

Structure-guided mutations in the cap-binding pocket of yeast Cbc2

An alignment of the primary structures of yeast Cbc2 and the 156-aa human CBP20 homolog highlights 101 positions

of amino acid side chain identity/similarity (Supplemental Fig. S1). Here, six of the conserved side chains in Cbc2 that comprise the m^7Gppp binding site in the crystal structure of human CBC (Fig. 1) were mutated to alanine. These were as follows: Tyr24, which stacks on the m^7G nucleobase and engages in hydrogen bonds with the β-phosphate of m^7Gppp and the ribose 2′OH; Asp120, which accepts a hydrogen-bond from the m^7G N1 atom; Asp122, which accepts a hydrogen-bond from the m^7G N2 atom; Arg129, which donates hydrogen bonds from its Nε and NH2 atoms to the cap ribose O3′ and O2′ atoms, respectively (and which also makes a bidentate salt bridge to Asp122); Arg133, which engages the β-phosphate of m^7Gppp; and Phe91, which is adjacent to the cap ribose. The alanine mutations were introduced into a plasmid-borne yeast *CBC2* gene under the control of its native promoter and then tested for activity in vivo in a *cbc2*Δ yeast strain, in parallel with a wild-type *CBC2* plasmid and an empty *CEN* vector. The *cbc2*Δ cells grew well on YPD agar at 34°C but were slow growing at 25°C, 30°C, and 37°C, as gauged by colony size. *cbc2*Δ cells failed to grow at 18°C and 20°C (Fig. 2A,B). Growth was restored at all temperatures after transformation of *cbc2*Δ with the wild-type *CBC2* plasmid. Each of the alanine mutants also supported growth of *cbc2*Δ cells at all temperatures tested (Fig. 2A,B).

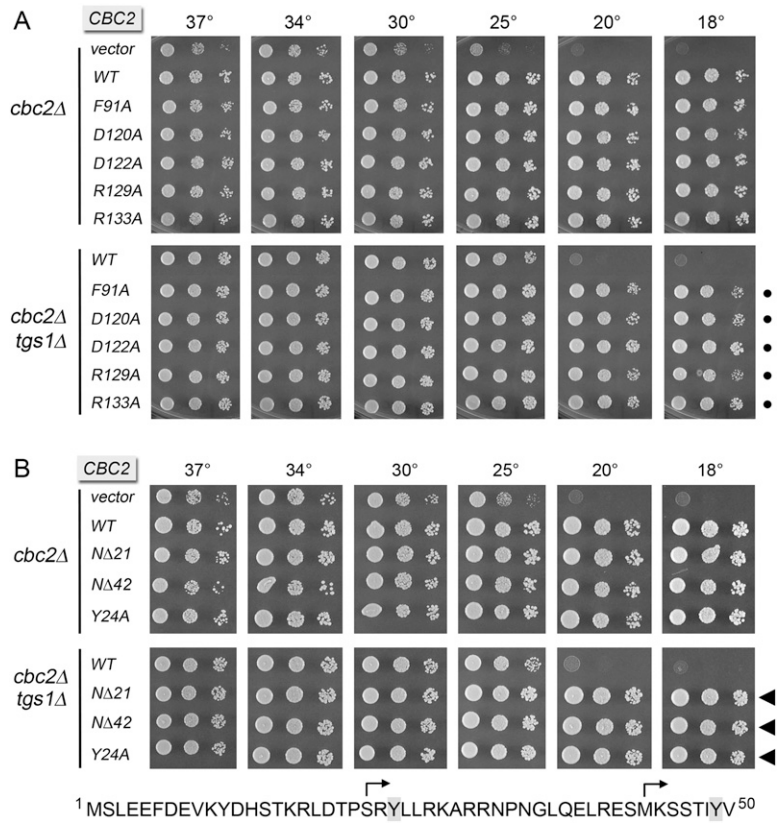

FIGURE 2. Effects of mutating the Cbc2 cap-binding pocket on yeast growth. (*A*) The phenotypes of *cbc2*Δ cells or *cbc2*Δ *tgs1*Δ cells harboring *CEN LEU2* plasmids with wild-type *CBC2* or the indicated mutant alleles were compared by spotting 3-μL aliquots of 10-fold serial dilutions of cells (from liquid cultures grown to mid-log phase at 34°C and adjusted to A_{600} of 0.1) to SD−Leu agar and incubating the plates at the indicated temperatures. Suppression of the *tgs1*Δ cs phenotype is denoted by • symbols at *right*. (*B*) The growth phenotypes of *cbc2*Δ and *cbc2*Δ *tgs1*Δ cells bearing *LEU2* plasmids with the indicated genes were assessed as described in panel *A*. Suppression of the *tgs1*Δ cs phenotype is denoted by ◀ symbols at *right*. The N-terminal amino acid sequence of Cbc2 is shown at the *bottom*, with the two m^7G-stacking tyrosines shaded gray and the margins of the N-terminal truncation mutants indicated by arrows.

In light of the structural evidence that the conformation of the N-terminal peptide segment of CBP20 is critical for formation of a proper cap binding site in human CBC (Calero et al. 2002; Mazza et al. 2002), we also tested the effects of deleting 21 or 42 amino acids from the N terminus of yeast Cbc2 (Fig. 2B). We found that the *NΔ21* and *NΔ42* alleles complemented the growth defects of *cbc2*Δ cells (Fig. 2B). These results suggest that an intact cap-binding pocket in yeast CBC is not required for apparently normal vegetative growth.

The benign effects of the above alanine and deletion mutations contrast with the overt growth defects of *cbc2*Δ cells (Fig. 2), which are similar to the growth defects of *sto1*Δ cells that lack the large subunit of yeast CBC (Fortes et al. 1999). An unexpected observation that a *sto1*Δ *cbc2*Δ double mutant grew better than either single mutant prompted the suggestion that production of either CBC subunit alone had a dominant negative effect on cell growth (Fortes et al. 1999). If that is the case, it complicates even further the issue of whether CBC subunits have cap-dependent and cap-independent functions. Thus, we revisited the issue, by mating *STO1 cbc2*Δ and *sto1*Δ *CBC2* haploids, sporulating the resulting heterozygous diploids, and dissecting the tetrads to score growth and genotype the haploid progeny. We obtained the expected outcomes of a two-gene cross, which yielded parental ditype (all four spores being slow-growing), nonparental ditype (two fast-growing wild-type progeny and two slow growing *sto1*Δ *cbc2*Δ progeny), and tetratype (one fast growing wild-type, two slow growing single mutants and one slow-growing double mutant) segregation patterns (Fig. 3A).

Freshly germinated *sto1*Δ *cbc2*Δ haploids cells were amplified briefly in liquid culture and then spotted in serial dilution on YPD agar in parallel with a wild-type sister strain: The double mutant was quite sick at 30°C, 34°C, and 37°C, as gauged by colony size, and did not grow at 20°C or 25°C

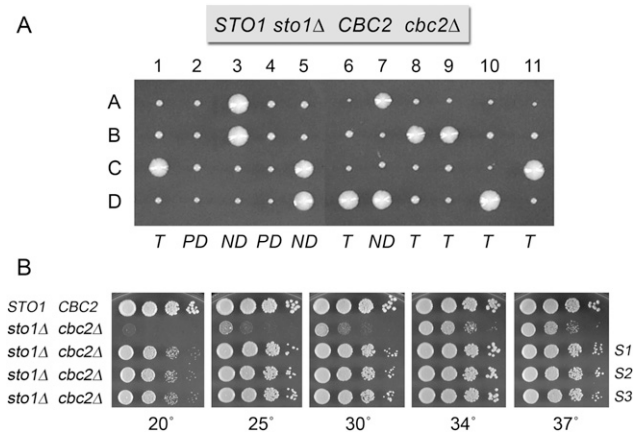

FIGURE 3. *sto1*Δ *cbc2*Δ double mutants give rise to spontaneous suppressors of slow growth. (*A*) Haploid progeny derived from tetrad dissection of a heterozygous diploid strain are shown. Spores from 11 tetrads were placed on YPD agar medium and incubated for 3 d at 30°C. The relevant genotype of the diploid is indicated at the *top*; A–D refers to colonies derived from sister spores; the segregation patterns of the markers for *sto1*Δ (hyg^R) and *cbc2*Δ (kan^R) are indicated *below* each tetrad: (T) tetratype, (PD) parental ditype, (ND) nonparental ditype. (*B*) The growth of wild-type cells was compared to that of *sto1*Δ *cbc2*Δ cells either taken from a colony immediately after germination or after continuous growth of individual haploids at 30°C and isolation of faster growing derivatives S1, S2, and S3. Cultures were adjusted to A_{600} of 0.1 and aliquots (3 μL) of serial dilutions were spotted to YPD agar. Plates were photographed after 2 d of incubation at 30°C, 34°C, and 37°C, 3 d at 25°C, or 5 d at 20°C.

(Fig. 3B). We noted that propagated cultures of *sto1*Δ *cbc2*Δ cells or *sto1*Δ cells plated on YPD agar yielded mixtures of small and large colonies. (This was not the case for *cbc2*Δ cells.) Whereas individually selected large colonies continued to yield homogeneously large colonies upon further propagation, the individually selected small colonies recapitulated the small/large dimorphism upon further growth. Three genetically independent large colony *sto1*Δ *cbc2*Δ derivatives (S1, S2, and S3, obtained from cultures of initially slow-growing *sto1*Δ *cbc2*Δ haploid progeny from different tetrad dissections) were tested for growth on YPD agar and were found to grow as well as wild type at 34°C and to display improved growth at all other temperatures vis à vis *sto1*Δ *cbc2*Δ, although S1, S2, and S3 were moderately cold-sensitive at 20°C compared to wild type (Fig. 3B). Similarly enhanced growth was seen for "large colony" derivatives of *sto1*Δ (data not shown). These findings indicate that *sto1*Δ *cbc2*Δ cells and *sto1*Δ cells readily acquire spontaneous mutations that suppress their vegetative growth defects. We suspect that the "better-growing" properties of the *sto1*Δ *cbc2*Δ strain used previously are attributable to an acquired suppressor mutation, which might complicate the interpretation of phenotypes observed in *sto1*Δ *cbc2*Δ or *sto1*Δ strains as being directly reflective of CBC function. This concern appears not to apply to *cbc2*Δ or the *cbc2* hypomorphs that we study presently.

Cbc2 cap binding site mutations suppress the cold-sensitivity of *tgs1*Δ cells

Tgs1, the enzyme that synthesizes TMG caps, is inessential for vegetative growth of *S. cerevisiae* (Mouaikel et al. 2002; Hausmann et al. 2008). *tgs1*Δ cells have no detectable TMG caps on their snRNAs, signifying that there is no Tgs1-independent route to form TMG caps. Despite the absence of TMG caps on their U1, U2, U4, and U5 snRNAs, *tgs1*Δ yeast cells display apparently normal steady state snRNA levels (Mouaikel et al. 2002) and no overt aberrations in the RNA or protein contents of their spliceosomal snRNPs, except for the acquisition of the nuclear CBC as a stoichiometric component of the U1 snRNP (Schwer et al. 2011). These findings indicated that the residual m^7G cap of the U1 snRNP in *tgs1*Δ cells is accessible to, and occupied by, nuclear CBC.

*tgs1*Δ cells fail to grow at 18°C and 20°C (Fig. 2A,B). We reported recently that the biologically active *cbc2-Y24A* allele completely suppressed the cold-sensitive growth defect caused by *tgs1*Δ (Schwer et al. 2011). This is evinced by transforming a viable *cbc2*Δ *tgs1*Δ double mutant with a plasmid bearing either wild-type *CBC2* or *cbc2-Y24A*. Whereas the *CBC2 tgs1*Δ strain was profoundly cold-sensitive, the *cbc2-Y24A tgs1*Δ strain grew as well as *TGS1* cells at 18°C and 20°C (Fig. 2B and data not shown). We inferred that the cold-sensitive phenotype of *tgs1*Δ is not caused by the lack of TMG caps per se but rather by the ectopic association, at low temperatures, of nuclear CBC with the m^7G cap of a normally TMG-capped U1 snRNA (Schwer et al. 2011). A corollary inference is that the capacity of otherwise benign Cbc2 mutations to suppress *tgs1*Δ cold-sensitivity can provide a genetic readout of diminished cap binding ability.

Thus, we transformed *cbc2*Δ *tgs1*Δ cells with the five other *cbc2-Ala* mutants (Fig. 2A) and the two N-terminal truncation mutants (Fig. 2B). In every case, growth at 18° and 20°C was restored. We surmise that the alanine substitutions for these cap binding side chains and the subtraction of the N-terminal 42-aa peptide (which includes the cap binding Tyr24 side chain) elicit genetically hypomorphic defects in cap binding by yeast CBC. To assess whether Cbc2 mutations affected the steady-state levels of Cbc2 in vivo, we performed Western blot analysis of whole-cell extracts of *cbc2*Δ and *cbc2*Δ *tgs1*Δ strains expressing TAP-tagged wild-type Cbc2, Cbc2-Ala, Cbc2-NΔ21, and Cbc2-NΔ42. The levels of immunoreactive Cbc2 were not diminished by the alanine mutations or the N-terminal deletions (Supplemental Fig. S2). The NΔ21 and NΔ42 polypeptides displayed expected incremental increases in electrophoretic mobility (Supplemental Fig. S2).

Cbc2-Y24A suppresses the requirement for Tgs1 in *PCH2* pre-mRNA splicing

A network of mutational synergies between *tgs1*Δ and yeast pre-mRNA splicing factors suggests that TMG caps facilitate

early steps in spliceosome assembly and that the effects of eliminating TMG caps on vegetative growth are buffered by other components of the splicing machinery (Hausmann et al. 2008; Chang et al. 2012). However, TMG caps are essential for yeast meiosis, where the absence of TMG caps in *tgs1*Δ cells causes a specific defect in the splicing of a subset of meiotic pre-mRNAs, including *PCH2* and *SAE3* (Qiu et al. 2011a,b). The Tgs1-dependence of the splicing of the *PCH2* pre-mRNA was attributed to a nonconsensus branchpoint sequence in the *PCH2* intron and an exceptionally long 5′ exon preceding the *PCH2* intron. Indeed, Tgs1-dependent expression of a *HIS3* reporter gene in vegetative cells could be achieved by inserting the *PCH2* intron at a distal site in the *HIS3* ORF (Qiu et al. 2011a,b). Here, we used the *HIS3*-[*PCH2*] reporter to query whether Tgs1-dependence might be circumvented by *cbc2-Y24A*. To do this experiment, we replaced the chromosomal *CBC2* gene with *cbc2-Y24A* in *TGS1* and *tgs1*Δ strains that carried the *HIS3*-[*PCH2*] cassette inserted at the chromosomal *HIS3* locus. The *HIS3*-[*PCH2*] gene was functional in *TGS1 CBC2* cells, as gauged by growth on agar medium lacking histidine, but not in *tgs1*Δ *CBC2* cells (Fig. 4A). The instructive finding here was that *HIS3*-[*PCH2*] function was restored in *tgs1*Δ *cbc2-Y24A* cells (Fig. 4A). We infer that ectopic binding of CBC to the U1 snRNA cap in *tgs1*Δ cells is responsible (at least in part) for the Tgs1-dependence of *PCH2* splicing. However, we found that *cbc2-Y24A* did not override the Tgs1 requirement for expression of a *HIS3*-[*SAE3*] reporter gene (data not shown).

To extend the analysis to true meiotic splicing, we replaced the chromosomal *CBC2* locus with *cbc2-Y24A* in yeast SKY cells that were either *TGS1* or *tgs1*Δ. (SKY, a derivative of SK1, is a strain of choice for studies of meiosis in light of its high efficiency and synchrony of sporulation.) Total RNA isolated from diploid wild-type, *tgs1*Δ, *cbc2-Y24A*, and *cbc2-Y24A tgs1*Δ SKY cells 8 h after transfer to sporulation medium was used as a template for oligo(dT)-primed reverse transcription (RT), followed by PCR amplification of the cDNA with oligonucleotide primers corresponding to exon sequences flanking the *PCH2* pre-mRNA intron (Fig. 4B). Agarose gel electrophoresis resolved the 214-bp DNA derived by RT-PCR amplification of the spliced *PCH2* mRNA from the 327-bp DNA derived from the unspliced *PCH2* transcript (Fig. 4B). As reported previously (Qiu et al. 2011b), *PCH2* meiotic splicing was defective in *tgs1*Δ cells, and the unspliced precursor was the predominant species seen after RT-PCR (Fig. 4B). The key finding was that *cbc2-Y24A* (which did not by itself affect meiotic splicing of the *PCH2* transcript) restored the wild-type pattern of efficient *PCH2* splicing in *tgs1*Δ cells undergoing sporulation (Fig. 4B). In contrast, the defect in *SAE3* pre-mRNA splicing in *tgs1*Δ cells undergoing meiosis was not reversed in *cbc2-Y24A tgs1*Δ cells (data not shown). Thus, not all effects of the loss of TMG caps on mRNA splicing can be ameliorated by weakening the Cbc2 cap binding site.

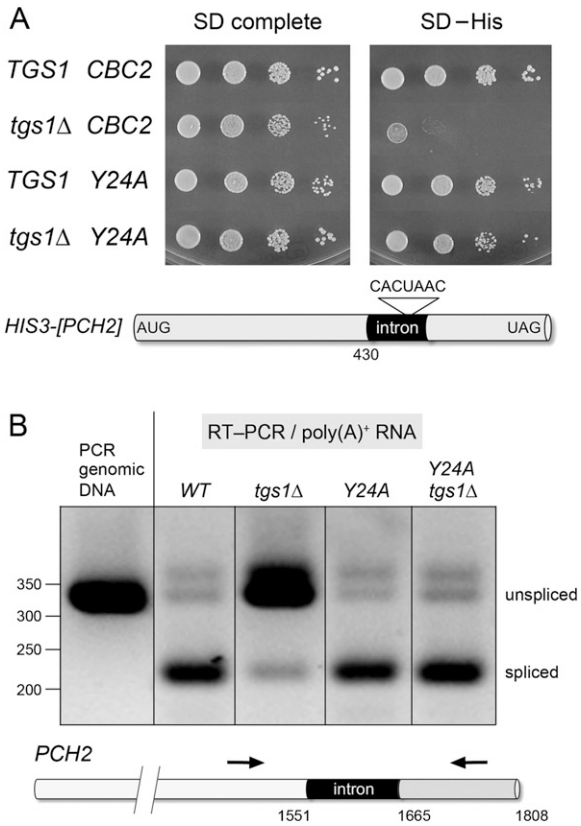

FIGURE 4. *cbc2-Y24A* suppresses the Tgs1-dependence of *HIS3*-[*PCH2*] expression and *PCH2* meiotic splicing. (*A*) Serial dilutions of yeast cells harboring the chromosomal *HIS3*-[*PCH2*] reporter gene were spotted in parallel on synthetic drop-out (SD) medium containing histidine (complete) or lacking histidine (–His) and incubated for 2 d at 30°C. The genotypes of the cells are indicated on the *left*. The *HIS3*-[*PCH2*] reporter is depicted at the *bottom*. The *HIS3* ORF is colored gray. The *PCH2* intron is colored black, and the nonconsensus branchpoint sequence is shown. (*B*) RNAs isolated from wild-type, *tgs1*Δ, *cbc2-Y24A*, and *cbc2-Y24A tgs1*Δ diploid SKY cells sampled 8 h post-transfer to sporulation medium were reverse transcribed with an oligo(dT) primer, and the cDNAs were PCR-amplified with primers flanking the intron of the chromosomal *PCH2* gene (depicted at the *bottom*). The PCR products were resolved by native agarose gel electrophoresis and visualized by staining with ethidium bromide (the negative image is shown). The *left* lane shows the product of PCR-amplification of genomic DNA with the *PCH2* primers, which is the same size as the RT-PCR product derived from the intron-containing *PCH2* pre-mRNA. The positions and sizes (bp) of linear duplex DNA markers are indicated on the *left*. The positions of the RT-PCR products of unspliced and spliced *PCH2* transcripts are indicated on the *right*.

Synthetic genetic interactions of Cbc2-Y24A with pre-mRNA splicing factors

The benign effect of Cbc2 cap binding site mutations on vegetative growth raises the prospect that the impact of these lesions, on splicing, for example, might be buffered by other actors in the splicing pathway. If so, then screening null alleles of vegetatively optional splicing factors for synthetic lethality or sickness with the hypomorphic allele

cbc2-Y24A might yield genetic insights more narrowly focused on cap-dependent functions of CBC than was the original screen for synthetic interactors with a *sto1*Δ *cbc2*Δ double mutant (Fortes et al. 1999).

We focused first on the U1 snRNP subunit Nam8 and the spliceosome assembly factor Mud2, mutations of which synergize with *sto1*Δ *cbc2*Δ (Fortes et al. 1999). *nam8*Δ and *mud2*Δ null mutations have no overt impact on yeast vegetative growth but are synthetically lethal with *tgs1*Δ (Hausmann et al. 2008). Here, we constructed haploid yeast strains amenable to tests of synthetic lethality by either plasmid shuffle or mating. For example, a haploid strain with chromosomal *cbc2-Y24A* and *mud2*Δ loci bearing a *MUD2* gene on a *CEN URA3* plasmid was unable to form colonies at 30°C or 37°C on agar medium containing FOA (5-fluoroorotic acid), a drug that selects against the *CEN URA3 MUD2* plasmid (Fig. 5A). Transformation of the *cbc2-Y24A mud2*Δ cells with *CEN LEU2* plasmids bearing either *MUD2* or *CBC2* enabled colony formation on FOA agar (Fig. 5A). These results signify that the otherwise benign Cbc2-Y24A mutation is lethal in the absence of Mud2.

A haploid *cbc2-Y24A nam8*Δ strain harboring a *CEN URA3 NAM8* plasmid was unable to form FOA-resistant colonies at 30°C but did at 37°C (Fig. 5A). Growth of *cbc2-Y24A nam8*Δ cells on FOA agar at 30°C was rescued by prior transformation with *CEN LEU2* plasmids bearing either *NAM8* or *CBC2* (Fig. 5A). Viable *cbc2-Y24A nam8*Δ cells selected on FOA at 37°C were then tested for growth on YPD agar; the double mutants grew slower than either single mutant at 37°C and did not grow at 30°C or 25°C (data not shown). Thus, the Cbc2-Y24A mutation is conditionally lethal in the absence of Nam8.

Mud1 is an inessential subunit of the yeast U1 snRNP. A *mud1*Δ null mutation has no vegetative growth phenotype, yet *mud1*Δ is synthetically lethal with *mud2*Δ and *nam8*Δ, and *mud1*Δ is synthetically sick with *tgs1*Δ (Abovich et al. 1994; Chang et al. 2010; Qiu et al. 2011a). Also, Fortes et al. (1999) identified *MUD1* in their screen for mutational synergy with *sto1*Δ *cbc2*Δ. Here, we mated *cbc2-Y24A MUD1* and *CBC2 mud1*Δ strains, sporulated the diploids, and dissected tetrads to recover *cbc2-Y24A mud1*Δ double mutants that germinated and grew at 30°C. We compared the growth of *cbc2-Y24A mud1*Δ cells on YPD agar to that of *CBC2 MUD1*, *cbc2-Y24A MUD1*, and *CBC2 mud1*Δ cells derived from the same cross. Whereas the single mutants grew as well as wild-type yeast at all temperatures tested, the *cbc2-Y24A mud1*Δ strain formed smaller colonies at 30°C and 34°C and failed to thrive at higher (37°C) or lower (20°C or 25°C) temperatures (Fig. 5B, top panel).

Swt21 is an inessential splicing factor that displays mutational synergies with Tgs1, the U1 snRNP subunit Prp40, and the CBC subunit Sto1 (Murphy et al. 2004; Hausmann et al. 2008; Hage et al. 2009). We mated *cbc2-Y24A SWT21* and *CBC2 swt21*Δ strains, sporulated the diploids, and dissected tetrads to recover viable *cbc2-Y24A swt21*Δ double mutants that were synthetically sick (at 25°C to 37°C) and cold-sensitive (at 20°C) compared to the single mutants, which grew as well as wild-type cells at 20°C–37°C (Fig. 5B, middle panel).

We also detected a synthetic growth defect when *cbc2-Y24A* was combined with *brr1*Δ or *ist3*Δ (Fig. 5B, bottom panel). Brr1 is an inessential splicing factor associated with U snRNPs that

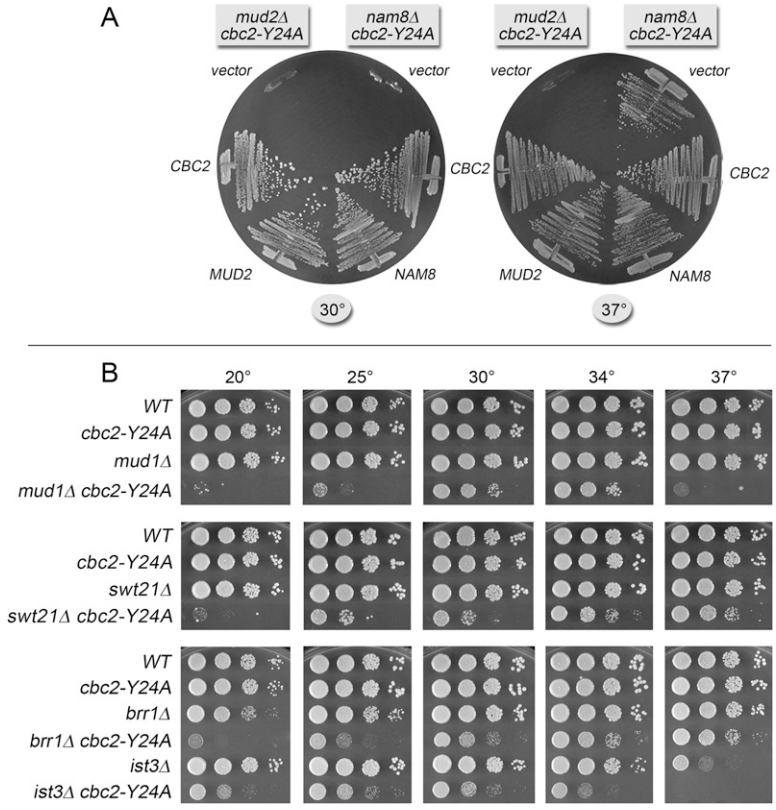

FIGURE 5. *cbc2-Y24A* is synthetic lethal with *mud2*Δ and *nam8*Δ and synthetic sick with *mud1*Δ, *swt21*Δ, *brr1*Δ, and *ist3*Δ. (*A*) Yeast *cbc2-Y24A mud2*Δ p360-MUD2 (*URA3 CEN MUD2*) or *cbc2-Y24A nam8*Δ p360-NAM8 (*URA3 CEN NAM8*) cells were transformed with *CEN LEU2* plasmids harboring wild-type *CBC2*, *MUD2*, or *NAM8* as specified. Leu^+ transformants were selected at 30°C and then streaked to agar medium containing 5-FOA (0.75 mg/mL). Cells transformed with the empty *LEU2* vector served as a negative control. The plates were photographed after 3 d of incubation at 30°C or 37°C. (*B*) Aliquots (3 μL) of serial 10-fold dilutions of haploid yeast strains of the specified genotypes were spotted on YPD agar medium. The plates were photographed after incubation for 2 d (30°C, 34°C, and 37°C), 3 d (25°C), or 5 d (20°C) as specified.

facilitates snRNP manufacture at low growth temperatures (Noble and Guthrie 1996). Yeast *brr1*Δ cells grow normally at 30°C–37°C but are slow-growing at 20°C. In contrast, the *brr1*Δ *cbc2-Y24A* double mutant failed to grow at 20°C, was extremely sick at 25°C and 30°C, and grew slower than either single mutant at 37°C (Fig. 5B, bottom panel). Ist3 is an inessential component of the U2 snRNP. An *ist3*Δ mutant grows well at 20°C–30°C but has a strong *ts* growth defect at 37°C. The *ist3*Δ *cbc2-Y24A* double mutant was sick at 20°C–34°C and inviable at 37°C (Fig. 5B, bottom panel).

Similar matings of *cbc2–Y24A* were performed with deletion mutants of yeast splicing factors Lea1 (a subunit of the U2 snRNP), Isy1 (a component of the NineTeen Complex that activates the spliceosome for catalysis), Cwc21 (a protein associated with the NineTeen Complex), and Swm2 ("synthetic with Mud2"). Viable double mutants were recovered after sporulation in all four instances, and we observed no synthetic growth defects of these double mutants when growth was tested at 20°C–37°C in parallel with the respective single mutants (data not shown).

We also tested for synthetic interactions of Cbc2-Y24A with proteins involved in RNA transactions other than pre-mRNA splicing, i.e., Lsm1 (mRNA decay), Pat1 (mRNA decay), Srb2 (RNA polymerase II transcription), and Rpn4 (transcription). We found no synthetic growth defects of the *lsm1*Δ *cbc2-Y24A*, *pat1*Δ *cbc2-Y24A*, *srb2*Δ *cbc2-Y24A*, or *rpn4*Δ *cbc2-Y24A* strains when growth was tested at 20°C–37°C in parallel with the respective single mutants (data not shown). Taken together, these results fortify the inferences that early steps of pre-mRNA splicing are the principal biological pathway impacted by the cap binding activity of yeast nuclear CBC.

Synthetic genetic interactions of Cbc2-Y24A with the yeast branchpoint binding protein Msl5

Saccharomyces cerevisiae Msl5 (branchpoint binding protein) orchestrates spliceosome assembly by binding the intron branchpoint sequence 5′-UACUAAC and establishing cross intron-bridging interactions with other components of the splicing machinery (Abovich et al. 1994; Abovich and Rosbash 1997; Rain et al. 1998; Rutz and Seraphin 1999; Wang et al. 2008; Chang et al. 2012). Unlike the optional splicing factors discussed above, Msl5 (a 476-aa polypeptide) is essential for yeast vegetative growth. The central branchpoint RNA binding domain of Msl5—composed of KH and QUA2 modules—is flanked by N- and C-terminal domains that have imputed functions in protein-protein interactions. By gauging the ability of Msl5 mutants to complement *msl5*Δ, we recently reported that the Mud2-binding (aa 35–54) and putative Prp40-binding ($PPxY^{100}$) elements of the Msl5 N-terminal domain are inessential, as are a C-terminal proline-rich domain (aa 382–476) and two zinc-binding CxxCxxxxHxxxxC motifs (aa 273–286 and 299–312) (Chang et al. 2012). A subset of conserved branchpoint RNA-binding amino acids in the central KH-QUA2 domain (aa 146–269) are essential, whereas other RNA-binding residues are dispensable. We used our collection of viable Msl5 mutants to illuminate synthetic genetic interactions between Msl5 and Mud2, Nam8, and Tgs1. The results suggested a network of important but functionally buffered protein–protein and protein–RNA interactions between the Mud2-Msl5 complex at the branchpoint and the U1 snRNP at the 5′ splice site (Chang et al. 2012). Here, we queried the genetic interactions of Cbc2-Y24A with our collection of Msl5 mutants that grow as well as wild-type *MSL5* cells.

The instructive findings were that *cbc2-Y24A* was synthetically lethal with otherwise benign mutations of amino acids Asn163, Val165, Val195, Lys196, Thr265, Arg267, Lys252, and Arg253 in the Msl5 KH-QUA2 domain (Table 1). The NMR structure of human branchpoint binding protein (SF1) bound to an RNA (5′-AUACUAACAA) containing the consensus yeast branchpoint sequence 5′-UAC UAAC (Liu et al. 2001) revealed an extensive network of contacts between many of these amino acids and the RNA nucleobases and sugars. The KH module engages the CUA**A**CAA-3′ segment of the RNA (the branchpoint adenosine is in bold). The QUA2 module binds to the proximal 5′-AUACU segment of the RNA. The KH residue Asn163 contacts the cytosine base and Val165 contacts the adenine base preceding the branchpoint adenosine. These contacts are inessential for *msl5*Δ complementation by the *N163A-V165A* mutant but are essential for viability in the *cbc2-Y24A* background at all temperatures tested (Table 1). The contacts

TABLE 1. Synthetic interactions of Cbc2-Y24A with Msl5

	*msl5*Δ *cbc2-Y24A* complementation			
MSL5 allele	18°C	25°C	30°C	37°C
WT	+++	+++	+++	+++
35-476	+++	+++	+++	+++
55-476	+	+++	+++	–
69-476	–	–	–	–
1-458	++	+++	+++	+++
1-437	+	+	+++	+++
1-425	+	+	+++	+
1-401	–	–	+	+
1-312	–	–	–	–
55-437	–	–	–	–
P97A P98A Y100A	–	–	–	–
N163A V165A	–	–	–	–
V195A K196A	–	–	+	++
T265A R267A	–	–	–	+
K252A R253A	–	–	–	–
K252R	–	–	–	++
R253K	+++	+++	+++	+++
C273A C276A	+++	+++	+++	+++
C299A C302A	+++	+++	+++	+++

of Lys196 with the adenine base preceding the branchpoint adenosine and of Val195 with the branchpoint adenine are also inessential for *msl5*Δ complementation, but the combination of *msl5-(V195A-K196A)* and *cbc2-Y24A* resulted in smaller colonies at 37°C (scored as ++), microcolonies at 30°C (scored as +), and no growth at 25°C or 18°C (Table 1). The RNA interactions of QUA2 residues Thr265 (a van der Waals contact with the ApC phosphate) and Arg267 (with the ribose 2′-OH and 3′-phosphate of the 5′-terminal adenosine and with the N6, C5, and N7 atoms of the downstream adenine) are not essential for *msl5*Δ complementation. However, the *msl5-(T265A-R267A) cbc2-Y24A* double mutant was barely viable at 37°C (+ growth) and failed to grow at 30°C, 25°C, or 18°C (Table 1). The QUA2 double mutant *K252A-R253A* was unconditionally synthetic lethal with *cbc2-Y24A*. Whereas the single mutant *K252R* was also synthetic lethal with *cbc2-Y24A* at 18°C–30°C (and synthetic sick at 37°C), the single mutant *R253K* had no mutational synergy with *cbc2-Y24A* (Table 1). These results highlight how CBC-cap- and Msl5-branchpoint interactions make genetically overlapping contributions to spliceosome assembly in vivo.

In contrast, there was no equivalent synthetic lethality of *cbc2-Y24A* with paired cysteine-to-alanine mutations in the putative zinc-binding residues of the two zinc-knuckle domains of yeast Msl5. The *C273A-C276A* and *C299A-C302A* mutations that disrupt the proximal and distal knuckles, respectively, had no effect on cell growth in the *cbc2-Y24A* background (scored as +++ in Table 1).

Otherwise benign incremental C-terminal deletions of Msl5 (*1-458*, *1-437*, *1-425*, and *1-401*) elicited a gradient of worsening synthetic sickness in the *cbc2-Y24A* background, culminating in unconditional lethality in the case of the *msl5-(1-312)* allele when combined with *cbc2-Y24A* (Table 1). Whereas deleting 34 aa from the N terminus of Msl5 had no apparent impact on yeast growth in *cbc2-Y24A*, extending the N-terminal deletion to 54 aa results in cold-sensitive (at 18°C) and temperature-sensitive (at 37°C) synthetic phenotypes (Table 1). Further deletion of the Msl5 segment from aa 55–68 resulted in unconditional synthetic lethality with *cbc2-Y24A* (Table 1). Insofar as the Msl5-(55-476) and Msl5-(69-476) mutants should be unable to form a heterodimeric complex with Mud2 (Wang et al. 2008), the mutational synergies of Cbc2-Y24A with the Msl5 N-terminal deletions are consistent with the lethality of *cbc2-Y24A* in the *mud2*Δ background (Fig. 5). Combining deletions of the terminal segments 1–54 and 438–458 (neither of which, per se, affected the growth of *cbc2-Y24A* at 30°C) resulted in unconditional lethality in the *cbc2-Y24A* background (Table 1). Msl5 contains a ^{97}PPxY^{100} motif recognized by WW domain proteins (Wiesner et al. 2002). Whereas a triple-alanine mutant *msl5-(P97A-P98A-Y100A)* fully complements *msl5*Δ, we find that this allele is unconditionally lethal in the *cbc2-Y24A* background (Table 1). In sum, these results reveal manifold genetic connections between CBC cap binding and the branchpoint binding protein that had not been appreciated previously.

Effects of Cbc2 cap binding site mutations on *SUS1* pre-mRNA splicing

The growth defects of *sto1*Δ and *cbc2*Δ null mutants are caused, at least in part, by aberrant histone modification, specifically increased histone H2B ubiquitylation (Hossain et al. 2009). A contributing factor is that splicing of the *SUS1* mRNA encoding a ubiquitin protease is reduced in *sto1*Δ and *cbc2*Δ cells. *SUS1* is one of the few yeast genes that contain two introns (Fig. 6), and it is the splicing of the first intron (which has nonconsensus 5′ splice site and branchpoint sequences) that is selectively impaired in the absence of CBC (Hossain et al. 2009). Here, we examined the effects of Cbc2 cap binding site lesions *Y24A* and *NΔ42* on the *SUS1* mRNA splicing pattern. Total RNA was isolated from *CBC2*, *cbc2*Δ, *cbc2-Y24A*, and *cbc2-NΔ42* cells grown in liquid culture at 30°C and used as a template for cDNA synthesis by reverse transcriptase primed by oligo(dT). The cDNA was then amplified by PCR with *SUS1* gene-specific primers corresponding to the sequences of exon 1 and exon 3 (Fig. 6). As reported previously (Hossain et al. 2009), the *SUS1* transcripts in wild-type *CBC2* cells consist predominantly of mature mRNA and a minority intermediate species in which the second intron is excised but the first intron is not (Fig. 6). In *cbc2*Δ cells, there is little mature mRNA, and the singly spliced intermediate comprises the predominant species, along with a significant fraction of unspliced pre-mRNA (Fig. 6). The salient findings were that (1) *cbc2-Y24A* cells evinced a wild-type pattern of *SUS1* splicing, and (2)

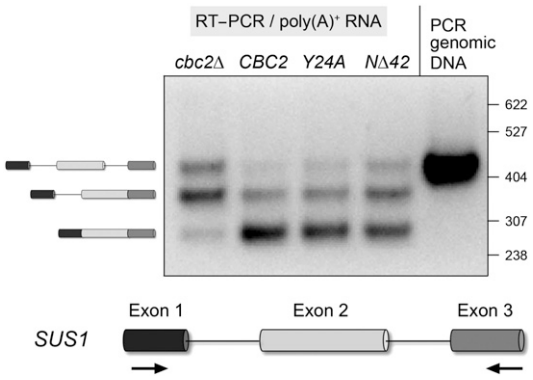

FIGURE 6. Effects of Cbc2 Y24A and NΔ42 mutations on *SUS1* pre-mRNA splicing. RNAs isolated from *cbc2*Δ, *CBC2*, *cbc2-Y24A*, and *cbc2-NΔ42* cells were reverse transcribed with an oligo(dT) primer, and the cDNAs were PCR-amplified with primers in the first and third exons of chromosomal *SUS1* gene (depicted at the *bottom*). The PCR products were resolved by native agarose gel electrophoresis and visualized by staining with ethidium bromide. The *right* lane shows the product of PCR-amplification of genomic DNA with the *SUS1* primers. The positions and sizes (bp) of linear duplex DNA markers are indicated on the *right*. The positions of the RT-PCR products of unspliced, partially spliced, and fully spliced *SUS1* transcripts are indicated at *left*.

cbc2-NΔ42 cells showed just a slight decrement in joining of the first and second exons (Fig. 6). These results underscore that mutations of the cap-binding pocket of Cbc2 exert hypomorphic effects on splicing that contrast with the more severe effects of ablating CBC.

Because the *SUS1* mRNA splicing defect is a straightforward molecular marker of the CBC null phenotype, it was of interest to gauge whether this defect was reversed in the *sto1*Δ *cbc2*Δ strains S1, S2, and S3 that displayed enhanced vegetative growth. Thus, we analyzed the *SUS1* splicing patterns by RT-PCR amplification of *SUS1* transcripts isolated from wild-type, *sto1*Δ, *sto1*Δ *cbc2*Δ, and the S1, S2, and S3 suppressor strains (Supplemental Fig. S3). The S1, S2, and S3 strains maintained a defective *SUS1* splicing pattern whereby the partially spliced RNA retaining the proximal intron was the predominant species (Supplemental Fig. S3). Yet, the S1, S2, and S3 strains did form slightly higher levels of the fully spliced *SUS1* transcript compared to that seen in the *sto1*Δ single mutant and the *sto1*Δ *cbc2*Δ double mutant, said levels still being much less than the mature *SUS1* transcript seen in wild-type *CBC2* cells (Supplemental Fig. S3). We surmise that the suppression of the CBC-null growth defect does not negate the CBC dependence of *SUS1* splicing.

The Cbc2 N-terminal peptide is critical for yeast sporulation and meiosis

The yeast meiotic developmental program entails a shift in the processing patterns of specific meiotic pre-mRNAs from a vegetative "off" state, in which single introns are included, to a meiotic "on" state, in which the target introns are removed. The efficiency of meiotic intron removal is either regulated or governed by the actions of splicing factors or RNA modifying enzymes that are inessential for vegetative growth (e.g., Mer1, Nam8, Tgs1) (Engebrecht et al. 1991; Spingola and Ares 2000; Munding et al. 2010; Qiu et al. 2011a,b,c). The yeast *sae1-1* mutation causes a severe sporulation defect in an otherwise wild-type background that is associated with a delay and decrement in meiotic recombination and a transient meiotic prophase arrest (McKee and Kleckner 1997). The wild-type *SAE1* gene was isolated from a genomic library by complementation of the *sae1-1* sporulation defect and then identified as *CBC2* (McKee and Kleckner 1997). Whereas the nature of the *sae1-1* mutation was not defined in the original study, our colleague Scott Keeney has since sequenced the *sae1-1* locus and found that it contains a single mutation at nucleotide +3 in the translation start codon: from AUG to AUA. The predicted impact of this change would be to shift the translation start site to the next available in-frame AUG encoding Met43 (Fig. 2), assuming that the scanning ribosome elides an intervening out-of-frame AUG at nucleotides 32–34 of the ORF. Having shown above that the Cbc2-(43-208) protein (NΔ42) sustains normal vegetative growth of haploid cells, we evaluated the effects of the *cbc2-NΔ42* allele on yeast sporulation, with the intent to create a "cleaner" version of *sae1-1*, uncomplicated by translational frame issues.

The sporulation experiments were performed in the SKY strain background. We monitored the appearance of four-spore asci as a function of time after transfer of a culture of yeast SKY diploid cells to sporulation medium. Wild-type SKY efficiently and synchronously formed asci between eight and 14 h and attained 86% and 90% sporulation efficiencies at 14 and 24 h, respectively (Fig. 7). In contrast, an isogenic *cbc2-NΔ42* diploid was defective in executing the meiotic program, with delayed onset and a slowed rate of ascus formation, to extents of only 5% and 19% after 14 and 24 h, respectively (Fig. 7). (The *sae1-1* mutant yielded 20% four-spore asci at 24 h [McKee and Kleckner 1997].) Spore viability was gauged by tetrad dissection (at the 24-h time point) and quantified as the percent of spores germinating to form macroscopic colonies after incubation for 3 d at 30°C on YPD agar medium. The spore viability values were 98% (310/316 viable spores) for the wild-type strain and 61% (413/676 viable spores) for the *cbc2-NΔ42* strain. We conclude that an intact cap binding site in Cbc2 is needed for yeast sporulation, presumably because a key meiotic RNA transaction is facilitated by CBC interactions with RNA caps.

We also tested the effects on sporulation of null mutants of two splicing factors—Mud2 and Swt21—that displayed mutational synergy with the hypomorphic *Y24A* mutant of Cbc2 during vegetative growth. The kinetics and extent of sporulation of the *swt21*Δ diploid were similar to that of the isogenic wild-type diploid (Fig. 7). In contrast, the *mud2*Δ diploid was defective for sporulation, yielding 12% and 22% asci at 14 and 24 h, respectively (Fig. 7).

Defective meiotic splicing of *SAE3* and *MER3* pre-mRNAs in *cbc2-NΔ42* cells

We isolated total RNA from *CBC2* and *cbc2-NΔ42* SKY diploids 4 h after transfer to sporulation medium. cDNA

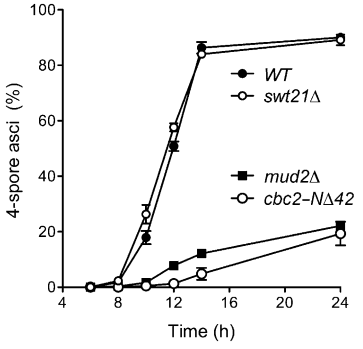

FIGURE 7. *cbc2-NΔ42* diploids are defective for sporulation. Homozygous wild-type, *swt21*Δ, *mud2*Δ, and *cbc2-NΔ42* SKY diploids were examined by light microscopy at the indicated times after transfer to sporulation medium. The percentages of the cell population comprising four-spore asci are plotted as a function of time.

was prepared from each RNA sample by reverse transcription primed by a mixture of antisense primers complementary to the 3′ exons of 14 meiotically spliced yeast mRNAs (Table 2). The cDNA preparations were then used as templates for gene-specific PCR amplification (Qiu et al. 2011a,b). The sense and antisense PCR primers corresponded to sequences flanking the introns so that the longer products of amplification of cDNA derived from unspliced pre-mRNAs could be easily resolved by native gel electrophoresis from the shorter products of amplification of cDNAs copied from spliced mRNA. The sense strand primer was 5′ ^{32}P-labeled in each PCR reaction so that we could quantify the distributions of unspliced and spliced cDNAs for each gene of interest. The results are compiled in Table 2, wherein each datum for splicing efficiency—[spliced/(spliced + unspliced)] × 100—is the average of three independent sporulation experiments and RT-PCR analyses. We operationally defined a significant mutational effect on meiotic splicing as one that elicits a greater than or equal to twofold reduction in splicing efficiency compared to a wild-type control (Qiu et al. 2011a,b). *SAE3* and *MER3* were the only two transcripts that met our criterion for a meiotic splicing defect in the *cbc2-NΔ42* strain. *SAE3* splicing efficiency was 81% in *CBC2* cells versus 20% in *cbc2-NΔ42*. *MER3* splicing efficiency was 79% in the *CBC2* cells versus 32% in *cbc2-NΔ42* (Table 2). In contrast, the *cbc2-NΔ42* mutation had no adverse effect on splicing of the *AMA1*, *MER2*, *HOP2*, *REC114*, *REC102*, *DMC1*, *PCH2*, *SPO1*, and *SRC1* transcripts (Table 2) and elicited only modest decrements in the splicing of *MEI4*, *SPO22*, and *MND1* that did not meet our criterion of significance (Table 2).

Rescue of the *cbc2-NΔ42* sporulation defect by expression of intronless cDNAs

The RNA analysis in Table 2 suggested that *SAE3* and *MER3* comprise a novel meiotic splicing "regulon" governed by Cbc2's cap binding activity. As shown previously (Qiu et al. 2011c), the working definition of a "complete" meiotic splicing regulon is the ability to rescue the sporulation defect caused by mutation of the splicing "governor" by expressing intronless cDNA versions of the essential meiotic RNAs that are targeted by the governor (which, in this case, are *SAE3* and *MER3*). Therefore, we introduced intronless *cSAE3* and *cMER3* (under the control of their native promoters) into the chromosomal *leu2*::*hisG* locus of *cbc2-NΔ42* SKY diploids and then assessed their sporulation efficiency. In parallel, we analyzed sporulation by *CBC2* diploids (positive control), *cbc2-NΔ42* diploids with no cDNAs (negative control), and *CBC2* diploids coexpressing *cSAE3* and *cMER3*. The ectopic cDNA genes had no negative impact on the kinetics of sporulation of *CBC2* cells (Fig. 8A). The salient finding was that the rate and extent of sporulation of the *cbc2-NΔ42* strain was restored fully to the wild-type pattern by coexpression of *cSAE3* and *cMER3* (Fig. 8A). The spore viability value after tetrad dissection was 95% for the *cbc2-NΔ42 + cSAE3 + cMER3* strain (148/156 viable spores) compared to 61% for *cbc2-NΔ42*. These results suggest that defective splicing of specific meiotic transcripts underlies the failure of *cbc2-NΔ42* cells to execute the meiotic program.

To further define the nature of the defect, we generated *cbc2-NΔ42* diploids bearing only *cMER3* or *cSAE3* inserted at the chromosomal *leu2*::*hisG* locus. The key finding was that expression of just the *MER3* cDNA sufficed to restore both the wild-type pattern of sporulation kinetics in the *cbc2-NΔ42* background (Fig. 8B) and a wild-type level of spore viability (92%; 218/236 viable spores). In contrast, *cbc2-NΔ42* cells expressing just the *SAE3* cDNA exhibited the same delay in the onset of sporulation seen in the parental *cbc2-NΔ42* strain and a slower rate of accrual of four-spore tetrads than that seen for the *CBC2* and *cbc2-NΔ42 + cMER3* strains (Fig. 8B). Nonetheless, *cSAE3* expression did enhance the rate of spore formation versus *cbc2-NΔ42*, such that the yield of four-spore asci at 24 h was 45% with *cSAE3* versus 22% without (Fig. 8B). However, the spore viability of the *cbc2-NΔ42 + cSAE3* strain was 60% (154/256 viable spores), i.e., the same as *cbc2-NΔ42*. Taken together, these experiments implicate *MER3* splicing as a limiting transaction in *cbc2-NΔ42* cells undergoing meiosis.

To evaluate whether the rescue of *cbc2-NΔ42* meiosis by ectopic expression of *cMER3* might simply reflect increased *MER3* gene dosage, we replaced the endogenous intron-containing chromosomal *MER3* locus of SK1 haploids with an intronless *MER3* cDNA, mated them to yield *cbc2-NΔ42 cMER3* diploids, and then analyzed their sporulation. The allelic replacement of *MER3* by *cMER3* fully restored wild-type sporulation kinetics (Fig. 9A), indicating that bypass of feeble *MER3* splicing in the *cbc2-NΔ42* background was responsible for the rescue of the meiotic defect.

TABLE 2. Meiotic mRNA splicing efficiency: Effects of *cbc2-NΔ42*

RNA	*CBC2* (% spliced)	*cbc2NΔ42* (% spliced)
AMA1	80 ± 8	95 ± 1
MER2	91 ± 3	93 ± 2
MER3	79 ± 8	32 ± 3
HOP2	87 ± 1	85 ± 3
REC114	88 ± 6	97 ± 1
MEI4	85 ± 9	52 ± 13
REC102	84 ± 2	84 ± 1
DMC1	99 ± 1	98 ± 1
PCH2	86 ± 5	95 ± 1
SAE3	81 ± 3	20 ± 1
SPO1	96 ± 1	92 ± 1
SPO22	98 ± 1	81 ± 1
MND1	94 ± 1	66 ± 1
SRC1	96 ± 1	94 ± 2

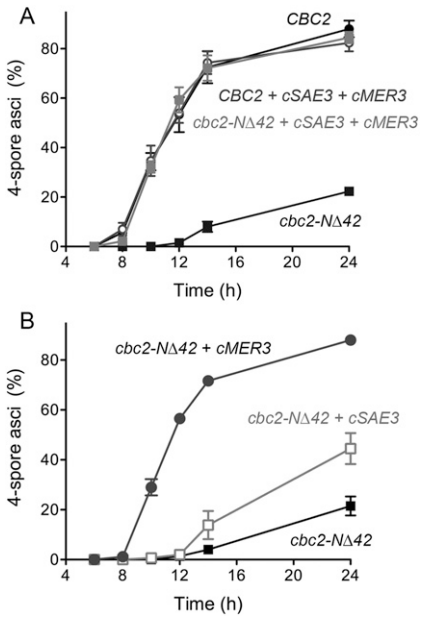

FIGURE 8. An ectopic *MER3* cDNA rescues the *cbc2-NΔ42* sporulation defect. (*A*) *CBC2* and *cbc2-NΔ42* diploids with or without the *cSAE3* and *cMER3* cDNAs integrated at the chromosomal *leu2*::*hisG* locus and (*B*) *cbc2-NΔ42* diploids and derivatives with either *cSAE3* or *cMER3* integrated at *leu2*::*hisG* were examined by light microscopy at the indicated times after transfer to sporulation medium. The percentages of the cell population comprising four-spore asci are plotted as a function of time.

Nonconsensus *MER3* intron features dictate the *cbc2-NΔ42* sporulation defect

MER3 splicing during yeast meiosis is known to be dependent on Mer1, a splicing enhancer protein that is produced only in meiotic cells (Engebrecht et al. 1991; Nakagawa and Ogawa 1999). *MER3*, together with *MER2*, *AMA1*, and *SPO22*, comprise a four-gene meiotic splicing regulon controlled by Mer1 and the vegetatively inessential U1 snRNP subunit Nam8 (Spingola and Ares 2000; Qiu et al. 2011a,c). Mer1 up-regulation of *MER3* splicing relies on the binding of the Mer1 protein to an enhancer element, 5′-ACACC CUU, located in the *MER3* intron next to the 5′ splice site (Fig. 9; Spingola and Ares 2000; Qiu et al. 2011a). The *MER3* intron has a nonconsensus 5′ splice site that is the decisive factor in Nam8/Mer1-dependency (Qiu et al. 2011a); two other members of the regulon (*MER2* and *SPO22*) also have nonconsensus 5′ splice sites that dictate their reliance on Mer1 and Nam8 (Nandabalan et al. 1993; Qiu et al. 2011a). In light of the present findings that *MER3* is the only member of the Mer1/Nam8 meiotic splicing regulon that is acutely sensitive to the *cbc2-NΔ42* mutation, we sought to identify the features of the *MER3* transcript that dictate this sensitivity.

Inspection of the *MER3* intron reveals two features not found in other Mer1/Nam8 targets: (1) a deviant 5′ splice site (GUAGUA) found in no other yeast intron; and (2) a rare nonconsensus branchpoint (GACUAAC) (Fig. 9). We initiated an analysis of the *cbc2-NΔ42* sensitivity of *MER3* splicing by installing consensus 5′ splice site (*5′SS* = GUAUGU) and branchpoint (*BP* = UACUAAC) signals in the *MER3* gene, singly and in combination (Fig. 9). These intron mutations were constructed in the *MER3* gene derived from yeast strain W303 (Qiu et al. 2011a). The W303 *MER3* intron differs from that of the SK1 strain by a single nucleobase change (T in SK1 versus C in W303) at a site between the branchpoint and the 3′ splice site (Fig. 9). Consequently, we also constructed a new control *MER3* SKY diploid strain (designated *WT** in Fig. 9) in which the W303 version of the *MER3* intron was introduced at the two chromosomal SK1 *MER3* loci. The single-base intron strain variation had no significant effect on the defective sporulation pattern of the *cbc2-NΔ42* strain (Fig. 9A). As expected, the viability of the *cbc2-NΔ42 MER3-WT** spores was compromised (48%; 30/80 viable spores).

The instructive finding was that introducing a perfect GUAUGU 5′ splice site (via a single U insertion, as shown in Fig. 9) restored wild-type sporulation kinetics in the *cbc2-NΔ42* strain (Fig. 9A) as well as spore viability (94%; 75/80 viable spores). The consensus *BP* change elicited a partial restoration of the sporulation pattern, albeit with a residual kinetic lag in the appearance of four-spore asci (Fig. 9A). Nonetheless, the viability of the spores derived from the *cbc2-NΔ42 MER3-BP* strain was 94% (75/80 viable spores). The effects of combining the *MER3 5′SS* and *BP* changes were virtually identical to those seen for the single *5′SS* change (Fig. 9A). These results signify that the aberrant *MER3* 5′ splice site and branchpoint are independent determinants of the sensitivity of *MER3* splicing to *cbc2-NΔ42*, with the 5′ splice site exerting an apparently greater influence in this regard.

To relate sporulation with *MER3* splicing, we performed RT-PCR analysis of the *MER3* transcripts in cells isolated 4 h after transfer to sporulation medium. As expected, control *CBC2* strains displayed high efficiencies of splicing of the *WT* and *WT** *MER3* transcripts (93%), whereas splicing was inefficient (33%) in *cbc2-NΔ42* cells (Fig. 9B). Installing a consensus 5′ splice site increased *MER3* splicing in *cbc2-NΔ42* cells to 99%. The consensus BP change elicited a lesser increase in *MER3* splicing, to 66% (Fig. 9B). Thus, the sporulation phenotype of *cbc2-NΔ42* cells correlates with the efficiency of *MER3* splicing.

DISCUSSION

The present genetic analysis of Cbc2 highlights phenotypic distinctions between null mutations and lesions of the cap-binding pocket of yeast CBC. Whereas *cbc2Δ*, *sto1Δ*, and *sto1Δ cbc2Δ* strains have similar vegetative growth defects, the latter two strains readily elaborate spontaneous suppressors. Although we have not determined the nature of the suppressor mutations, prior studies have documented

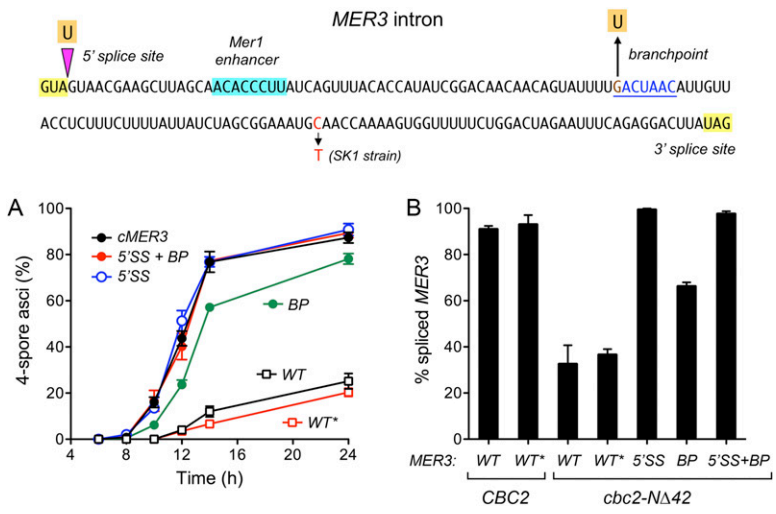

FIGURE 9. Nonconsensus *MER3* intron features dictate the *cbc2-NΔ42* sporulation defect. The nucleotide sequence of the *MER3* intron of yeast strain W303 is shown, highlighting its nonconsensus 5′ splice site and branchpoint and the location of its Mer1 enhancer (shaded in cyan). The point mutations (*5′SS* and *BP*) that we introduced into the *MER3* intron are indicated. A single C-to-T difference in the *MER3* intron of the yeast SK1 strain (from which SKY is derived) is highlighted in red. (*A*) *cbc2-NΔ42* diploids with the indicated chromosomal *MER3* alleles were examined by light microscopy at the indicated times after transfer to sporulation medium. The percentages of the cell population comprising four-spore asci are plotted as a function of time. (*B*) RNAs isolated from the indicated diploid *CBC2* or *cbc2-NΔ42* SKY strains (with chromosomal *MER3* alleles as specified) at 4 h post-transfer to sporulation medium were reverse transcribed with a *MER3* antisense primer complementary to the 3′ exon. The cDNAs were then PCR-amplified with sense and antisense primers flanking the *MER3* intron. The splicing efficiencies are plotted; each datum is the average of three separate experiments ±SEM.

that the *sto1*Δ growth defect can be overcome by directed mutations that block histone H2B ubiquitylation (Hossain et al. 2009). *cbc2*Δ mutants appear (qualitatively) less prone to acquire spontaneous growth-restoring suppressors, which simplifies our comparison of the null phenotypes to those elicited by structure-guided mutations of the cap binding site.

A consistent finding was that alanine mutations and N-terminal deletions predicted to weaken the Cbc2-cap interaction (according to the structures of human CBC-cap complexes and available functional studies of cap binding by human CBC mutants) (Calero et al. 2002; Mazza et al. 2002; Worch et al. 2009) had no impact on vegetative growth. The genetic behavior of these alleles with respect to suppression of the *tgs1*Δ cold-sensitivity fortifies the inference that these are hypomorphs that restore growth of *tgs1*Δ at low temperatures because they ameliorate the ectopic binding of CBC to the U1 snRNA m^7G cap. The phenotypes of the cap binding hypomorphs of Cbc2 are distinct from those accompanying mutations that are predicted to abolish cap binding, i.e., *Y24A-Y49A*, which eliminates both of the conserved tyrosines that form the π-cation sandwich around the m^7G nucleobase (Fig. 1). To wit, *cbc2-Y24A-Y49A* cells have a profound cold-sensitive growth defect at 20°C, 25°C, and 30°C (Supplemental Fig. S4A) similar to *cbc2*Δ (Fig. 2), and the *cbc2-Y24A-Y49A* allele does not suppress *tgs1*Δ cold-sensitivity (Supplemental Fig. S4A), notwithstanding that the steady-state levels of Cbc2-Y24A-Y49A are similar to wild-type Cbc2 (Supplemental Fig. S4B). A plausible conclusion from these findings is that budding yeast tolerates a decrement in cap binding by CBC but is sensitive to elimination of cap binding function.

The synthetic genetic interactions of *cbc2-Y24A* with *nam8*Δ, *mud1*Δ, *swt21*Δ, *mud2*Δ, *ist3*Δ, and *brr1*Δ and with multiple viable *msl5* alleles make clear that the decrement in cap binding by CBC is buffered by yeast proteins that act during the early steps of spliceosome assembly, entailing recruitment of U1 snRNP to the 5′ splice site and the Mud2/Msl5 complex to the intron branchpoint, with the establishment of cross-intron bridging contacts between them (Abovich et al. 1994; Abovich and Rosbash 1997; Rain et al. 1998; Rutz and Seraphin 1999; Wang et al. 2008; Chang et al. 2012). The genetics of this cap binding hypomorph are consistent with, and lend further support to, the imputed role of CBC binding to the pre-mRNA cap in stabilizing the U1 snRNP at the 5′ splice site (Colot et al. 1996; Lewis et al. 1996; Görnemann et al. 2005; Hage et al. 2009). In an otherwise wild-type background, a weakened cap binding site in CBC seems to support adequate levels of splicing of the many intron-containing pre-mRNAs needed for vegetative growth. This is in keeping with our findings that the kinetics and efficiency of splicing of yeast *ACT1* and *RP51A* pre-mRNAs in a yeast in vitro system are unaffected by the absence of an m^7G cap on the pre-mRNA and the depletion of the yeast capping enzyme Ceg1 (Schwer and Shuman 1996). It is likely that the m^7G mRNA cap and its engagement by CBC are important for splicing a subpopulation of yeast intron-containing transcripts. *SUS1* is a two-intron-containing yeast transcript that relies on CBC for splicing of its noncanonical proximal intron (Fig. 6; Hossain et al. 2009), but we find here that mutations of the Cbc2 cap-binding pocket do not recapitulate the strong *SUS1* splicing defect seen in *cbc2*Δ cells.

The finding that a deletion of the N-terminal 42-aa peptide of Cbc2 significantly compromises yeast meiosis and sporulation (while having no impact on vegetative growth) confirms and extends the studies of *sae1-1* (McKee and Kleckner 1997). Our analysis shows that splicing of the *MER3* and *SAE3* meiotic pre-mRNAs is impaired by *cbc2-NΔ42* mutation, implying that processing of these transcripts

during meiosis is especially dependent on the binding of CBC to the pre-mRNA cap. Although *MER3* and *SAE3* splicing are affected to similar degrees by *cbc2-NΔ42*, the cDNA rescue experiments revealed that *MER3* is the biologically vulnerable transcript. The meiotic defect of *cbc2-NΔ42* can be fully overcome by expression of an intronless *MER3* cDNA but not by an intronless *SAE3* cDNA. The sensitivity of sporulation and of *MER3* splicing to *cbc2-NΔ42* is conferred by nonconsensus intronic 5′ splice site and branchpoint sequences, with the unusual 5′ splice site playing a larger role, as surmised from the degree to which the sporulation/splicing defects were rectified by installing a consensus splicing signal. The effects of *cbc2-NΔ42* on meiotic *MER3* splicing fortify the inferences from the synthetic genetic interactions in vegetative cells that CBC acts during the early spliceosome assembly and reveal the gene-specific nature of the requirement for full cap binding activity by CBC during splicing.

Meiosis-specific pre-mRNA splicing in budding yeast embraces multiple pre-mRNA targets grouped into regulons defined by their genetic requirements for vegetatively optional splicing factors (e.g., splicing enhancer Mer1 and the U1 snRNP subunit Nam8) or snRNA modifications (trimethylguanosine caps synthesized by Tgs1). The present identification of *MER3* and *SAE3* as constituents of a meiotic splicing regulon governed by Cbc2 adds a new dimension to the picture (Supplemental Fig. S5), especially the overlap of the pre-mRNA clients of the various splicing factors. For example, *MER3* belongs to two different splicing regulons: Mer1/Nam8 and Cbc2. *SAE3* also belongs to two regulons: Tgs1 and Cbc2. Our findings here that yeast sporulation is defective in the absence of splicing factor Mud2 (which has no effect, per se, on vegetative growth) hints at the existence of yet another meiotic regulon. Collectively, these results highlight an untapped reservoir of genetic connections between pre-mRNA splicing and yeast meiosis.

MATERIALS AND METHODS

CBC knockout strains

To obtain *sto1Δ cbc2Δ* cells, we first generated a *sto1Δ* haploid strain in which the *STO1* open reading frame between positions +1 and +2525 was replaced with the *hygMX* cassette (Goldstein and McCusker 1999). Correct targeting of the *STO1* locus was confirmed by diagnostic Southern blotting. Yeast *sto1Δ* cells (α *his3Δ1 leu2Δ0 met15Δ0 ura3Δ0 sto1Δ::hygMX*) were mated with *cbc2Δ* cells (**a** *his3Δ1 leu2Δ0 met15Δ0 ura3Δ0 cbc2Δ::kanMX*) (Chang et al. 2010) to yield heterozygous diploids *STO1 sto1Δ CBC2 cbc2Δ* that were resistant to G418 and hygromycin. The diploids were sporulated, tetrads were dissected, and the segregation pattern of the marker genes *hygMX* and *kanMX* was determined by replica plating on drug-containing medium.

Cbc2 mutants and tests of their function

Plasmid pRS415-CBC2-TAP (*CEN LEU2*) expresses a Cbc2-TAP fusion protein under the transcriptional control of the native *CBC2* promoter (Schwer et al. 2011). Single-alanine mutations Y24A, F91A, D120A, D122A, R129A, and R133A, double alanine mutation Y24A-Y49A, and N-terminal truncations NΔ21 and NΔ42 were introduced into Cbc2-TAP by PCR amplification of the ORF with mutagenic primers. The mutated DNA fragments were digested with BamHI and XmaI and inserted into pRS415-CBC2-TAP in lieu of the wild-type *CBC2-TAP* gene. The inserts in each of the pRS415-based plasmids were sequenced completely to confirm that no unwanted coding changes were acquired during amplification and cloning. To assay the function of wild-type and mutated *CBC2* alleles, isogenic *cbc2Δ* and *cbc2Δ tgs1Δ* cells (Chang et al. 2010) were transfected with the empty *CEN LEU2* vector (pRS415) or pRS415-CBC2-TAP plasmids. Individual Leu^+ transformants were selected at 34°C and then grown in liquid culture in SD–Leu medium at 34°C. The cultures were adjusted to A_{600} of 0.1 and aliquots (3 μL) of serial 10-fold dilutions were spotted on SD–Leu agar. The plates were incubated at 18°C, 20°C, 25°C, 30°C, 34°C, and 37°C.

Allelic replacements at the chromosomal *CBC2* locus

Targeting cassettes for replacement of the chromosomal *CBC2* locus by wild-type *CBC2-TAP–hygMX*, *cbc2-Y24A-TAP–hygMX* and *cbc2-Y24A-Y49A-TAP–hygMX* were generated by inserting *hygMX* between the stop codon of *CBC2-TAP* and a segment of genomic DNA 3′ from the *CBC2* ORF within the respective pRS415-CBC2-TAP plasmids. DNA fragments encompassing (1) a 550-bp segment homologous to genomic *CBC2* sequences upstream of the start codon, (2) the wild-type or mutated *CBC2-TAP* ORF, and (3) the hygromycin-resistance gene and a 390-bp segment of DNA homologous to *CBC2* sequences downstream from the stop codon were excised and transfected into wild-type and *tgs1Δ* yeast cells (Hausmann et al. 2008). Hyg^R transformants were selected, and the allelic replacements were confirmed by diagnostic PCR, Southern blotting, and sequencing of the chromosomal *CBC2* ORF after amplification by PCR.

Impact of *cbc2-Y24A* on the Tgs1-dependence of *HIS3*-[*PCH2*] reporter gene expression

The chromosomal *HIS3*-[*PCH2*] reporter gene in which the *PCH2* intron is inserted at position 430 within the *HIS3* ORF requires splicing of the *PCH2* intron to confer histidine prototrophy (Qiu et al. 2011a,b). Yeast reporter strains *TGS1 CBC2 HIS3*-[*PCH2*], *tgs1Δ CBC2 HIS3*-[*PCH2*], *TGS1 cbc2-Y24A HIS3*-[*PCH2*], and *tgs1Δ cbc2-Y24A HIS3*-[*PCH2*] were grown in liquid YPD medium until the cultures attained A_{600} of 0.6–1.0. Cells (1 A_{600} unit) were harvested by centrifugation, washed once in water, and then resuspended in 1 mL of water. Aliquots (3 μL) of serial 10-fold dilutions were spotted to SD and SD–His agar medium, and the plates were incubated at 30°C.

Impact of *cbc2-Y24A* on the Tgs1-dependence of meiotic mRNA splicing

Haploid SKY163 (*MAT*a *ho::LYS2 lys2 ura3 leu2::hisG*) and SKY164 (*MAT*α *ho::LYS2 lys2 ura3 leu2::hisG*) strains were transfected with the *cbc2-Y24A-TAP–hygMX* integration cassette. Hyg^R transformants were selected, and the allelic replacements were confirmed by diagnostic Southern blotting. The SKY163 *cbc2-Y24A* and SKY164 *cbc2-Y24A* haploids were mated, and

homozygous *cbc2-Y24A* diploids were identified based on their inability to mate with tester strains. The *cbc2-Y24A* haploids were also mated to *tgs1Δ::kanMX* and *tgs1Δ::natMX* SKY strains (Qiu et al. 2011b); the diploids were sporulated, tetrads were dissected, and SKY haploids *cbc2-Y24A–hygMX tgs1Δ::kanMX* and *cbc2-Y24A–hygMX tgs1Δ::natMX* were recovered. These were then mated to obtain homozygous *cbc2-Y24A tgs1Δ* diploids. To assess meiotic *PCH2* splicing, cultures of wild-type, *tgs1Δ*, *cbc2-Y24A*, and *tgs1Δ cbc2-Y24A* SKY diploids were grown, and sporulation was induced as described previously (Qiu et al. 2011a,b,c). RNA was extracted from cells harvested 8 h after transfer to sporulation medium by using the hot acidic phenol method (Collart and Oliviero 1993). After treatment with DNase I, aliquots (2 μg) of the RNA preparations were used for oligo(dT_{23})-primed cDNA synthesis by reverse transcriptase which was performed with the Protoscript kit (New England Biolabs) according to the vendor's instructions. Aliquots comprising 4% of the RT reaction mixture served as templates to PCR-amplify the *PCH2* cDNAs with primers 5′-GCATAGAGGAGATGATAACTTCAGGT (sense) and 5′-CCA GAACAAACTCATCGTCGTCTAC (antisense) corresponding to sequences flanking the *PCH2* intron (Qiu et al. 2011a). The PCR products were resolved by electrophoresis through a native 2% agarose gel and visualized by staining with ethidium bromide. Control PCRs with equivalent aliquots of mock-RT reactions (in which reverse transcriptase was omitted) were performed in parallel, and these served to verify that the RNA preparations were free of genomic DNA. PCR of yeast genomic DNA with the same primers yielded a DNA fragment that served as a marker for RT-PCR of the unspliced *PCH2* transcript.

Tests of synthetic genetic interactions of *cbc2-Y24A*

Haploid *cbc2-Y24A–hygMX* cells were crossed to *mud2Δ*, *nam8Δ*, *mud1Δ*, *swt21Δ*, *ist3Δ*, *cwc21Δ*, *isy1Δ*, *swm2Δ*, *lea1Δ*, *brr1Δ*, *srb2Δ*, *lsm1Δ*, *pat1Δ*, and *rpn4Δ* (Hausmann et al. 2008; Chang et al. 2010). The heterozygous diploids were sporulated, tetrads were dissected, and spores were germinated at 30°C to obtain the desired double mutants *cbc2-Y24A mud1Δ*, *cbc2-Y24A swt21Δ*, *cbc2-Y24A ist3Δ*, *cbc2-Y24A cwc21Δ*, *cbc2-Y24A isy1Δ*, *cbc2-Y24A swm2Δ*, *cbc2-Y24A lea1Δ*, *cbc2-Y24A brr1Δ*, *cbc2-Y24A srb2Δ*, *cbc2-Y24A lsm1Δ*, *cbc2-Y24A pat1Δ*, and *cbc2-Y24A rpn4Δ*. Wild-type cells and the single and double mutants were grown in liquid culture in YPD medium. The cultures were adjusted to A_{600} of 0.1, and aliquots (3 μL) of serial 10-fold dilutions were spotted on YPD. The plates were incubated at 20°C, 25°C, 30°C, 34°C, and 37°C. We did not recover viable *cbc2-Y24A mud2Δ* or *cbc2-Y24A nam8Δ* haploids at 30°C, signifying that *cbc2-Y24A* was synthetic lethal with *mud2Δ* and *nam8Δ*. By introducing *CEN URA3 MUD2* and *CEN URA3 NAM8* plasmids (Chang et al. 2010; Qiu et al. 2011a) into the respective heterozygous diploids prior to sporulation and tetrad dissection, we were able to obtain viable *mud2Δ cbc2-Y24A* p[*CEN URA3 MUD2*] and *nam8Δ cbc2-Y24A* p[*CEN URA3 NAM8*] strains. However, they were unable to grow at 30°C on medium containing 5-FOA, a drug that selects against the complementing *URA3* plasmid.

Mutational synergies of *cbc2-Y24A* with mutations in the yeast branchpoint binding protein

Yeast *cbc2-Y24A msl5Δ* p316-MSL5 (*URA3 CEN MSL5*) cells were transfected with *CEN LEU2* plasmids bearing wild-type *MSL5* or various biologically active *msl5* mutant alleles described previously (Chang et al. 2012). Individual Leu^+ transformants were streaked on agar medium containing 1 mg/mL 5-FOA. Growth was scored after incubation for 7 d at 18°C, 25°C, 30°C, or 37°C. Synthetic lethal *msl5* mutants were those that failed to form colonies at any temperature. Individual FOA-resistant *cbc2-Y24A* colonies with viable *msl5* alleles were grown to mid-log phase in YPD broth and adjusted to A_{600} of 0.1. Aliquots (3 μL) of serial 10-fold dilutions were spotted on YPD agar plates, which were then incubated at 18°C, 25°C, 30°C, and 37°C. Growth was assessed as follows (see Table 1): (+++) Colony size was indistinguishable from strains bearing wild-type *MSL5*; (++) slightly reduced colony size; (+) only pinpoint macroscopic colonies were formed; (–) no growth.

Assay of *SUS1* splicing by RT-PCR

Yeast *cbc2Δ* cells that had been transformed with pRS415-CBC2-TAP plasmids (encoding wild-type Cbc2 or mutants Y24A or NΔ42) or with the empty pRS415 vector were grown in liquid SD−Leu medium until A_{600} reached 0.6–0.8. The cells (20 A_{600} units) were harvested by centrifugation, and total cellular RNA was recovered by using a Qiagen RNA isolation kit according to the vendor's instructions. The RNA preparations were treated with DNase I, and first-strand cDNA synthesis was carried out using the Protoscript Kit with oligo(dT_{23}) primers. Aliquots of the mixtures were then used for PCR amplification of the *SUS1* cDNA using primers (5′-TGGATACTGCGCAATTAAAGAGTC and 5′-TCATTGTGTATCTACAATCTCTTCAAG) complementary to the first and third exons (Hossain et al. 2009). The PCR products were resolved by electrophoresis through a native 2% agarose gel and visualized by staining with ethidium bromide.

Effects of *cbc2-NΔ42, mud2Δ,* and *swt21Δ* on yeast sporulation

SKY163 haploid cells were transfected with the *cbc2-NΔ42-TAP–hygMX* allelic replacement cassette or with gene-knockout cassettes *mud2Δ::kanMX* or *swt21Δ::kanMX*. SKY164 haploid cells were transfected with *cbc2-NΔ42-TAP–hygMX, mud2Δ::natMX*, or *swt21Δ::natMX*. After selection for drug-resistance, the targeted insertions were confirmed by diagnostic Southern blotting. Haploids were mated, and homozygous *mud2Δ* and *swt21Δ* diploids were selected on YPD agar containing 100 μg/mL nourseothricin and 150 μg/mL geneticin. *cbc2-NΔ42* diploids were identified based on their inability to mate with tester strains. Single colonies of the wild-type and mutant SKY diploid yeast strains were patched on agar plates with glycerol as the carbon source for at least 6 h to select for cells with healthy mitochondria. Cells were streaked on YPD agar plates and incubated for 2 d at 30°C. Single colonies were then inoculated into YPD liquid medium and grown at 30°C to stationary phase (A_{600} of 6–8). Aliquots were inoculated into 12.5 mL of presporulation medium (0.5% yeast extract, 1% peptone, 0.67% yeast nitrogen base [without amino acids], 1% potassium acetate, 0.05 M potassium biphthalate [pH 5.5], 0.002% antifoam 204) to attain an A_{600} of 0.8. The cultures were incubated for 7 h at 30°C and added to 100 mL of fresh presporulation medium to attain an A_{600} of 0.025 (for wild-type, *mud2Δ*, and *swt21Δ* strains) or 0.1 (for *cbc2-NΔ42*). These cultures were incubated for 16 h until A_{600} reached >2.0. The cells were harvested by centrifugation, washed twice with sporulation medium

(2% potassium acetate, 0.001% polypropylene glycol), and then resuspended in sporulation medium at A_{600} of 6. Aliquots were withdrawn from synchronous meiotic cultures at 6, 8, 10, 12, 14, and 24 h post-transfer to sporulation medium. The cells were fixed in an equal volume of 100% ethanol and then examined by light microscopy (100× magnification) to assess the abundance of four-spore asci. Two hundred cells from each sample were scored. The extents of sporulation (% asci) were plotted as a function of time in Figures 7–9. Each datum is the average of three separate experiments ±SEM.

Splicing of meiotic pre-mRNAs in *cbc2-NΔ42* diploids undergoing attempted sporulation

CBC2 and *cbc2-NΔ42* SKY diploids were induced to sporulate as described above. Total RNA was isolated from cells 4 h after transfer to sporulation medium and, after treatment with DNase I, used as a template for cDNA synthesis primed by a mixture of antisense primers complementary to the 3′ exons of 14 meiotically spliced yeast mRNAs (Qiu et al. 2011a,b). The cDNAs derived from the 14 known spliced meiotic transcripts were then PCR-amplified in reaction mixtures containing an unlabeled gene-specific antisense strand primer and a 5′-^{32}P-labeled gene-specific sense strand primer. The detailed RT-PCR methods and the sequences of the primers flanking the introns of the genes of interest were as reported previously (Qiu et al. 2011a). The RT-PCR products were analyzed by native polyacrylamide gel electrophoresis. An aliquot of a PCR amplification reaction using yeast genomic DNA as a template provided a marker for the unspliced species. The ^{32}P-labeled RT-PCR products derived from the unspliced and spliced RNA transcripts were visualized and quantified by scanning the dried gels with a Fuji BAS-2500 imager. The splicing efficiencies (% spliced = spliced/(spliced + unspliced) × 100) are compiled in Table 2, wherein each datum is the average of three separate experiments ±SEM.

Introduction of *SAE3* and *MER3* cDNAs at the *leu2::hisG* locus

The *cSAE3* and c*MER3* genes, consisting of the intronless *SAE3* and *MER3* cDNAs plus flanking segments of genomic DNA, were described previously (Qiu et al. 2011c). The c*SAE3* and c*MER3* genes were restricted at terminal sites and inserted individually or in tandem (with *cSAE3* upstream of *cMER3*) into yeast integrative vector pRS305 (*LEU2*) to yield pRS305-cSAE3, pRS305-cMER3, and pRS305-cSAE3-cMER3. These plasmids and the empty pRS305 vector were linearized by digestion with AgeI and then transfected, individually, into *CBC2* and *cbc2-NΔ42* SKY strains. Leu$^+$ transformants were selected, and integration of the cDNA-containing fragments (or empty vector fragments) into the *leu2::hisG* genomic loci was verified by diagnostic PCR.

Allelic replacements at the *MER3* locus

MER3 variants containing a consensus 5′ splice site (*5′SS*), a consensus branchpoint (*BP*), or both (*5′SS+BP*) were described previously (Qiu et al. 2011a). Targeting cassettes for allelic replacement of the chromosomal *MER3* locus were constructed in pBluescript-KS plasmids as follows: (1) The G418-resistance gene *kanMX* or the nourseothricin-resistance gene *natMX* was cloned into pKS-Bluescript between NotI (5′ end) and BamHI (3′ end) restriction sites to yield pBS-kanMX and pBS-natMX; (2) a DNA segment 3′ from the chromosomal *MER3* gene (from nucleotides 289 to 666 downstream from the *MER3* translation stop codon) was amplified by PCR from *S. cerevisiae* genomic DNA and then inserted between the BamHI and XhoI sites of pBS-kanMX and pBS-natMX to generate pBS-kanMX-3′MER3 and pBS-natMX-3′MER3; (3) genes *MER3*, *MER3-5′SS*, *MER3-BP*, *MER3-5′SS+BP* and *cMER3*, flanked by 435 bp of 5′ genomic DNA (immediately upstream of the *MER3* start codon) and 288 bp of 3′ genomic DNA (immediately downstream from the stop codon), were cloned between the SacII and NotI sites of pBS-kanMX-3′MER3 and pBS-natMX-3′MER3. The resulting cassettes comprised a tandem array of 5′-*MER3* flanking DNA, a *MER3* gene, and a 3′-*MER3* flanking DNA with an inserted selectable *kanMX* or *natMX* marker. The various *MER3–kanMX* and *MER3–natMX* cassettes were excised from the plasmids with SacII and XhoI. *MER3–kanMX* DNAs were transfected into *CBC2* and *cbc2-NΔ42 MAT*a SKY strains, and G418-resistant integrants were selected. The *MER3–natMX* DNAs were transfected into *CBC2* and *cbc2-NΔ42 MAT*α SKY strains, and nourseothricin-resistant integrants were selected. The targeted allelic replacements were confirmed by diagnostic PCR and sequencing of the chromosomal *MER3* gene. The haploids were then mated, and homozygous diploids were selected on YPD agar containing nourseothricin and G418.

SUPPLEMENTAL MATERIAL

Supplemental material (Figs. S1, S2, S3, S4, and S5) is available for this article.

ACKNOWLEDGMENTS

We thank Olivia Orta for technical assistance. This work was supported by US National Institutes of Health grants GM52470 (S.S.) and GM50288 (B.S.). S.S. is an American Cancer Society Research Professor.

Received April 8, 2012; accepted August 3, 2012.

REFERENCES

Abovich N, Rosbash M. 1997. Cross-intron bridging interactions in the yeast commitment complex are conserved in mammals. *Cell* **89:** 403–412.

Abovich N, Liao XC, Rosbash M. 1994. The yeast MUD2 protein: An interaction with PRP11 defines a bridge between commitment complexes and U2 snRNP addition. *Genes Dev* **8:** 843–854.

Calero G, Wilson KF, Ly T, Rios-Steiner JL, Clardy JC, Cerione RA. 2002. Structural basis of m^{7}GpppG binding to the nuclear cap-binding protein complex. *Nat Struct Biol* **9:** 912–917.

Chang J, Schwer B, Shuman S. 2010. Mutational analyses of trimethylguanosine synthase (Tgs1) and Mud2: Proteins implicated in pre-mRNA splicing. *RNA* **16:** 1018–1031.

Chang J, Schwer B, Shuman S. 2012. Structure-function analysis and genetic interactions of the yeast branchpoint binding protein Msl5. *Nucleic Acids Res* **40:** 4539–4552.

Collart MA, Oliviero S. 1993. Preparation of yeast RNA. *Curr Protoc Mol Biol* **23:** 13.12.1–13.12.5.

Colot HV, Stutz F, Rosbash M. 1996. The yeast splicing factor Mud13p is a commitment complex component and corresponds

to CBP20, the small subunit of the nuclear cap-binding complex. *Genes Dev* **10:** 1699–1708.

Engebrecht J, Voelkel-Meiman K, Roeder GS. 1991. Meiosis-specific RNA splicing in yeast. *Cell* **66:** 1257–1268.

Fortes P, Kufel J, Fornerod M, Polycarpou-Schwarz M, Lafontaine D, Tollervey D, Mattaj IW. 1999. Genetic and physical interaction involving the yeast nuclear cap-binding complex. *Mol Cell Biol* **19:** 6543–6553.

Goldstein AL, McCusker JH. 1999. Three new dominant drug resistance cassettes for gene disruption in *Saccharomyces cerevisiae*. *Yeast* **15:** 1541–1553.

Görnemann J, Kotovic KM, Hujer K, Neugebauer KM. 2005. Cotranscriptional spliceosome assembly occurs in a stepwise fashion and requires the cap binding complex. *Mol Cell* **19:** 53–63.

Hage R, Tung L, Du H, Stands L, Rosbash M, Chang TH. 2009. A targeted bypass screen identifies Ynl187p, Prp42p, Snu71p, and Cbp80p for stable U1 snRNP/pre-mRNA interaction. *Mol Cell Biol* **29:** 3941–3952.

Hausmann S, Shuman S. 2005. Specificity and mechanism of RNA cap guanine-N2 methyltransferase (Tgs1). *J Biol Chem* **280:** 4021–4024.

Hausmann S, Ramirez A, Schneider S, Schwer B, Shuman S. 2007. Biochemical and genetic analysis of RNA cap guanine-N2 methyltransferases from *Giardia lamblia* and *Schizosaccharomyces pombe*. *Nucleic Acids Res* **35:** 1411–1420.

Hausmann S, Zheng S, Costanzo M, Brost RL, Garcin D, Boone C, Shuman S, Schwer B. 2008. Genetic and biochemical analysis of yeast and human cap trimethylguanosine synthase: Functional overlap of TMG caps, snRNP components, pre-mRNA splicing factors, and RNA decay pathways. *J Biol Chem* **283:** 31706–31718.

Hossain MA, Claggett JM, Nguyen T, Johnson TL. 2009. The cap binding complex influences H2B ubiquitination by facilitating splicing of the *SUS1* pre-mRNA. *RNA* **15:** 1515–1527.

Hugouvieux V, Kwak JM, Schroeder JI. 2001. An mRNA cap binding protein, ABH1, modulate early abscisic acid signal transduction in *Arabidopsis*. *Cell* **106:** 477–487.

Izaurralde E, Lewis J, McGuigan C, Jankowska M, Darzynkiewicz E, Mattaj IW. 1994. A nuclear cap binding protein complex involved in pre-mRNA splicing. *Cell* **78:** 657–668.

Izaurralde E, Lewis J, Gamberi C, Jarmolowski A, McGuigan C, Mattaj IW. 1995. A cap-binding protein complex mediating U snRNA export. *Nature* **376:** 709–712.

Laubinger S, Sachsenberg T, Zeller G, Busch W, Lohmann JU, Rätsch G, Weigel D. 2008. Dual roles of the nuclear cap-binding complex and SERRATE in pre-mRNA splicing and microRNA processing in *Arabidopsis thaliana*. *Proc Natl Acad Sci* **105:** 8795–8800.

Lewis JD, Izaurralde E, Jarmolowski A, McGuinan C, Mattaj IW. 1996. A nuclear cap-binding complex facilitates association of U1 snRNP with the cap-proximal 5′ splice site. *Genes Dev* **10:** 1683–1698.

Liu Z, Luyten I, Bottomley MJ, Messias AC, Houngninou-Molango S, Sprangers R, Zanier K, Krämer A, Sattler M. 2001. Structural basis for recognition of the intron branch site RNA by splicing factor 1. *Science* **294:** 1098–1102.

Maquat LE, Tarn WY, Isken O. 2010. The pioneer round of translation: Features and funtions. *Cell* **142:** 368–374.

Mazza C, Segref A, Mattaj IW, Cusack S. 2002. Large-scale induced fit recognition of an m^7GpppG cap analogue by the human nuclear cap-binding complex. *EMBO J* **21:** 5548–5557.

McKee AHZ, Kleckner N. 1997. Mutations in *Saccharomyces cerevisiae* that block meiotic prophase chromosome metabolism and confer cell cycle arrest at pachytene identify two new meiosis-specific genes *SAE1* and *SAE3*. *Genetics* **146:** 817–834.

Mouaikel J, Verheggen C, Bertrand E, Tazi J, Bordonné R. 2002. Hypermethylation of the cap structure of both yeast snRNAs and snoRNAs requires a conserved methyltransferase that is localized to the nucleolus. *Mol Cell* **9:** 891–901.

Munding EM, Igel AH, Shiue L, Dorighi KM, Trevino LR, Ares M. 2010. Integration of a splicing network within the meiotic gene expression program of *Saccharomyces cerevisiae*. *Genes Dev* **24:** 2693–2704.

Murphy MW, Olson BL, Siliciano PG. 2004. The yeast splicing factor Prp40p contains functional leucine-rich nuclear export signals that are essential for splicing. *Genetics* **166:** 53–65.

Nakagawa T, Ogawa H. 1999. The *Saccharomyces cerevisiae MER3* gene, encoding a novel helicase-like protein, is required for crossover control in meiosis. *EMBO J* **18:** 5714–5723.

Nandabalan K, Price L, Roeder GS. 1993. Mutations in U1 snRNA bypass the requirement for a cell type–specific RNA splicing factor. *Cell* **73:** 407–415.

Noble SM, Guthrie C. 1996. Transcriptional pulse–chase analysis reveals a role for a novel snRNP-associated protein in the manufacture of spliceosomal snRNPs. *EMBO J* **15:** 4368–4379.

Papp I, Mur LA, Dalmadi A, Dulai S, Koncz C. 2004. A mutation in the cap binding protein 20 gene confers drought tolerance to *Arabidopsis*. *Plant Mol Biol* **55:** 679–686.

Qiu ZR, Schwer B, Shuman S. 2011a. Determinants of Nam8-dependent splicing of meiotic pre-mRNAs. *Nucleic Acids Res* **39:** 3427–3445.

Qiu ZR, Shuman S, Schwer B. 2011b. An essential role for trimethylguanosine RNA caps in *Saccharomyces cerevisiae* meiosis and their requirement for splicing of *SAE3* and *PCH2* meiotic pre-mRNAs. *Nucleic Acids Res* **39:** 5633–5646.

Qiu ZR, Schwer B, Shuman S. 2011c. Defining the Mer1 and Nam8 meiotic splicing regulons by cDNA rescue. *RNA* **17:** 1648–1654.

Raczynska KD, Simpson CG, Ciesiolka A, Szewc L, Lewandowska D, McNicol J, Szweykowska-Kulinska Z, Brown JWS, Jarmolowski A. 2010. Involvement of the nuclear cap-binding protein complex in alternative splicing in *Arabidopsis thaliana*. *Nucleic Acids Res* **38:** 265–278.

Rain JC, Rafi Z, Legrain P, Krämer A. 1998. Conservation of functional domains involved in RNA binding and protein–protein interactions in human and *Saccharomyces cerevisiae* pre-mRNA splicing factor SF1. *RNA* **4:** 551–565.

Rutz B, Seraphin B. 1999. Transient interaction of BBP/ScF1 and Mud2 with the splicing machinery affects the kinetics of spliceosome assembly. *RNA* **5:** 819–831.

Schwer B, Shuman S. 1996. Conditional inactivation of mRNA capping enzyme affects yeast pre-mRNA splicing in vivo. *RNA* **2:** 574–583.

Schwer B, Erdjument-Bromage H, Shuman S. 2011. Composition of yeast snRNPs and snoRNPs in the absence of trimethylguanosine caps reveals nuclear cap binding protein as a gained U1 component implicated in the cold-sensitivity of *tgs1*Δ cells. *Nucleic Acids Res* **39:** 6715–6728.

Spingola M, Ares M. 2000. A yeast intronic splicing enhancer and Nam8p are required for Mer1p-activated splicing. *Mol Cell* **6:** 329–338.

Topisirovic I, Svitkin YV, Sonenberg N, Shatkin AJ. 2011. Cap and cap-binding proteins in the control of gene expression. *Wiley Interdiscip Rev RNA* **2:** 277–298.

Visa N, Izaurralde E, Ferreira J, Daneholt B, Mattaj IW. 1996. A nuclear cap-binding complex binds Balbiani ring pre-mRNA cotranscriptionally and accompanies the ribonucleoprotein particle during nuclear export. *J Cell Biol* **133:** 5–14.

Wang Q, Zhang L, Lynn B, Rymond BC. 2008. A BBP–Mud2p heterodimer mediates branchpoint recognition and influences splicing substrate abundance in budding yeast. *Nucleic Acids Res* **36:** 2787–2798.

Wiesner S, Stier G, Sattler M, Macias MJ. 2002. Solution structure and ligand recognition of the WW domain pair of the yeast splicing factor Prp40. *J Mol Biol* **324:** 807–822.

Worch R, Jankowska-Anyszka M, Niedzwiecka A, Stepinski J, Mazza C, Darzynkiewicz E, Cusack S, Stolarski R. 2009. Diverse role of three tyrosines in binding of the RNA 5′ cap to the human nuclear cap binding complex. *J Mol Biol* **385:** 618–627.